REVIEWS OF GEOPHYSICS, VOL. 24, NO. 4, PAGES 833–874, NOVEMBER 1986

Intermediate and Deep Seismicity and Lateral Structure of Subducted Lithosphere in the Circum-Pacific Region

G. VANNESS BURBACH[1] AND CLIFF FROHLICH

Institute for Geophysics and Department of Geological Sciences, University of Texas at Austin

In this paper we present a region-by-region review of the Wadati-Benioff zone structure of most of the world's seismically active subduction zones, focusing primarily on the intermediate and deep seismicity. Lateral changes in Wadati-Benioff zone structure are common in every major subduction zone. In this study we use these changes to define possible boundaries between portions or "segments" of lithosphere with differing subduction geometries. Although earthquake data seldom have the resolution to show conclusively whether these boundaries separate independent blocks of lithosphere, the available data indicate that the active process at most of these segment boundaries is ductile deformation of the subducting plate, rather than tearing. We found the strongest evidence for the existence of tears where tears are geometrically necessary, such as where a transform boundary terminates a trench, as at the New Hebrides, Tonga, and South Sandwich Trenches. Weak evidence suggesting other tears does exist in some regions, such as Taiwan, the Japan/Izu-Bonin corner, and the Philippines. The causes of these changes in structure are, in most cases, unclear. Only about 34% of the possible segment boundaries coincide with subducting bathymetric features. Some boundaries occur where there is apparent lateral strain caused by anomalous trench geometry. We have designed a simple modeling procedure which incorporates published plate motion and the observed geometry of trenches and Wadati-Benioff zones to estimate the lateral strain in subduction zones throughout the circum-Pacific region. Although no observed subduction zone has a perfectly strain-free geometry, there is a broad range of geometries for which the lateral strain is small. Indeed, the observed geometry of most subduction zones involve relatively little lateral strain. Comparison with centroid moment tensor focal mechanisms indicates that in zones where the modeling predicted little lateral strain, the mechanisms of intermediate and deep earthquakes show no effects of lateral stress, and downdip stresses are clearly dominant. In regions such as the Mariana Arc, where the model predicts very large lateral extension, lateral tension is very evident in the focal mechanisms. In regions such as the Hokkaido corner, where the modeling predicts large compressional strains, the plate appears to buckle, and bending stresses parallel to the trench are evident. In general this study finds that subducted lithosphere is remarkably cohesive and rigid, and only rarely deforms by breaking or stretching.

CONTENTS

[1]Now at Shell Western E. & P., Inc., P.O. Box 576, Houston, xas 77001.

ber number 6R0298.
55-1209/86/006R-0298$15.00

INTRODUCTION

Most studies of Wadati-Benioff zones have focused on the two-dimensional structure perpendicular to the trench. This paper will address two major problems involving aspects of the three-dimensional structure of subduction zones. The first problem concerns the lateral strain that arises when a plate that is essentially a spherical shell subducts along an irregular trench. The second problem concerns the significance of abrupt changes in structure along the strike of a trench, and whether these changes reflect lateral segmentation.

Isacks and Molnar [1971] reviewed the focal mechanisms of intermediate and deep earthquakes and concluded that most reflect the presence of downdip stresses in the plane of the subducting plate. *Forsyth and Uyeda* [1975] and *Chapple and Tullis* [1977] argued that the negative buoyancy of subducting lithosphere provides the primary driving mechanism of plate tectonics. However, downdip stresses do not explain all the observed focal mechanisms in some regions [*Fujita and Kanamori*, 1981; *Vassiliou*, 1984; *Vassiliou et al.*, 1984].

Frank [1968] and others [*Strobach*, 1973; *Tovish and Schubert*, 1978] have shown that, for thin subducting spherical shells, the surface area is conserved only if the radius of curvature of the arc is equal to twice the dip of the subducting slab. Any other geometry will produce either lateral stretching or lateral shortening of the plate as it is subducted. The present study will address several important questions about lateral strain. How much lateral strain of the subducted lithosphere do observed Wadati-Benioff zone geometries require? How does the subducted lithosphere accommodate this lateral strain? How does the lateral strain affect the observed seismicity and focal mechanisms?

Several investigators have proposed that subducted lithosphere is broken into numerous independent blocks separated by tears or hinge faults [*Stoiber and Carr*, 1973; *Carr et al.*, 1973; *Veith*, 1974]. However, *Isacks and Barazangi* [1977] found no clear evidence for such tears in most arcs. *Bevis and Isacks* [1984] used trend-surface analysis to study the Wadati-Benioff zone structure in several regions, and reached much the same conclusion. *Yamaoka et al.* [1986] used inextensible vinyl shells fit to plaster models of subduction zones to show that most observed subduction geometries can be fit with relatively little lateral strain. They found it necessary to introduce tears in only a few places.

Some of the disagreement about the extent of lateral segmentation has occurred because most previous investigators did not precisely define what a "segment" is. For some, a segment is a physically independent, specific block of subducted lithosphere that is separated from segments on either side by tears or hinge faults. For others, a segment means simply some arbitrarily delineated portion of a subducting plate that they wish to discuss.

For this study, there are three important questions about segmentation. Where are the changes in structure or seismicity that might constitute segment boundaries? How are these changes accommodated, for example, by tears, or ductile deformation? What are the causes of segmentation?

We will address the problems of lateral strain and segmentation in the context of a global review of the intermediate and deep structure of subducted lithosphere. To delineate the three-dimensional structure of subducted lithosphere, we use teleseismic locations of earthquakes with depths constrained by *pP* phases, and three-dimensional computer graphics, along with conventional analysis methods.

To address the problem of lateral strain, we have developed a simple modeling method to estimate the strain expected for the lithosphere defined by the observed Wadati-Benioff zone geometries. These estimated strains are often consistent with published centroid moment tensor focal mechanisms. Where the predicted lateral strains are small, downdip stresses dominate the focal mechanisms almost entirely. Where the predicted lateral strain is large, there are often many events with laterally oriented stress axes. Where the simple models predict great lateral extension, as in the Mariana Arc, lateral tension dominates the focal mechanisms. Where the models predict great lateral compression, such as at the Hokkaido corner, the subducting plate appears to buckle, and bending stresses perpendicular to the direction of convergence are dominant.

To address the problem of segmentation, we carefully examine the teleseismic data for specific characteristics or patterns which might indicate a change in structure. We have designated the locations of these characteristics as "possible segment boundaries" (PSBs) and we compare them to changes in other features such as volcanism, and to tears and segment boundaries proposed by previous investigators. While the teleseismic data seldom have the resolution to completely rule out tears, analysis of these data and published data from local networks indicates that most major changes in structure probably involve continuous contortions rather than discrete tears. We find strong evidence of hinge faulting only where the plate geometry requires it, such as where a trench meets a transform boundary, or where there is a reversal in the polarity of subduction. However, there is weak evidence of tears in some other regions.

The causes of segmentation are usually not clear. In some cases the subduction of bathymetric features is important, but such features occur at fewer than half of the observed PSBs. In a few cases, lateral strain due to trench geometry may contribute to segmentation.

The first part of this paper will describe the data and methods used in this study (Figures 1-3), and will define the terminology we use. The second part discusses the scientific problems, and presents the major conclusions of this study (Figures 4-8). The results themselves are presented in the form of regional summaries at the end of the paper (Figures 9-20). The appendix presents a detailed explanation of the modeling method.

DATA AND METHODS

Seismicity Data and Focal Mechanisms

The primary data for this study are all earthquakes reported by the International Seismological Center (ISC) between 1964 and 1980 which had focal depths constrained by *pP-P* intervals (ISC-*pP* data) (Figure 1). Because depth is the most critical location parameter, as well as the most difficult to determine accurately, the use of events with *pP-f*(PIP depths is important. Some *pP* phases are actually reflections off the sea surface; thus some *pP-P* depths may have systematic errors. However, these errors will be smaller than the uncertainties in depths determined with *P* phases alone. The ISC-*pP* data discriminate against shallow events since shallow events seldom have clear *pP* phases, but there are enough shallow events with *pP-P* constraint in most areas to adequately define the shallow structure of the Wadati-Benioff zones.

In addition to the ISC-*pP* data, we also examined historical seismicity data reported in the International Seismological Summary and the ISC, including all events of reported surface wave magnitude 7.0 or above with depths of over 70 km occurring between the years 1900 and 1963. We did not use the historical data directly to determine the structure of the Wadati-Benioff zones; rather, we used them as a measure of the completeness on the ISC-*pP* data, particularly where the ISC-*pP* data were scarce.

The focal mechanisms used in this study are the double couples that best fit the centroid moment tensors (CMT) published by the Harvard group [*Giardini*, 1984; *Dziewonski and Woodhouse*, 1983; *Dziewonski et al.*, 1983*a*, *b*, *c*, 1984*a*, *b*, *c*] for the period from January 1977 to August 1984. These focal mechanisms are likely to be of more consistent quality than those derived from first-motion studies. For each region we present all the mechanisms for events with focal depths of 70 km or greater, except for the Alaska-Aleutian Arc, Lesser Antilles Arc, and the Scotia Arc, for which we include the mechanisms of all events deeper than 50 km. In each region,

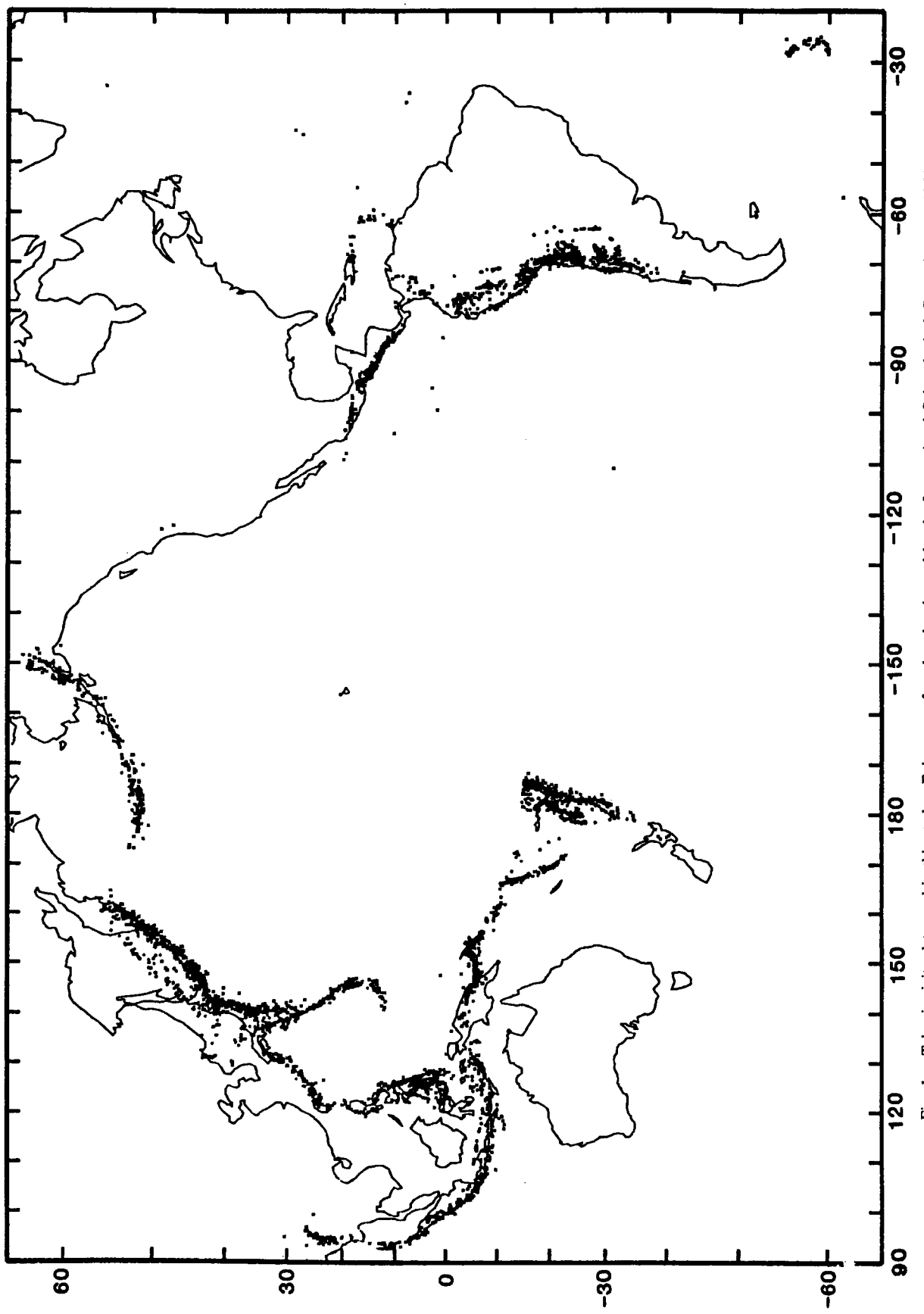

Fig. 1. Teleseismicity data used in this study. Epicenters of earthquakes located by the International Seismological Center between 1964 and 1980 which had reported *pP-P* depths.

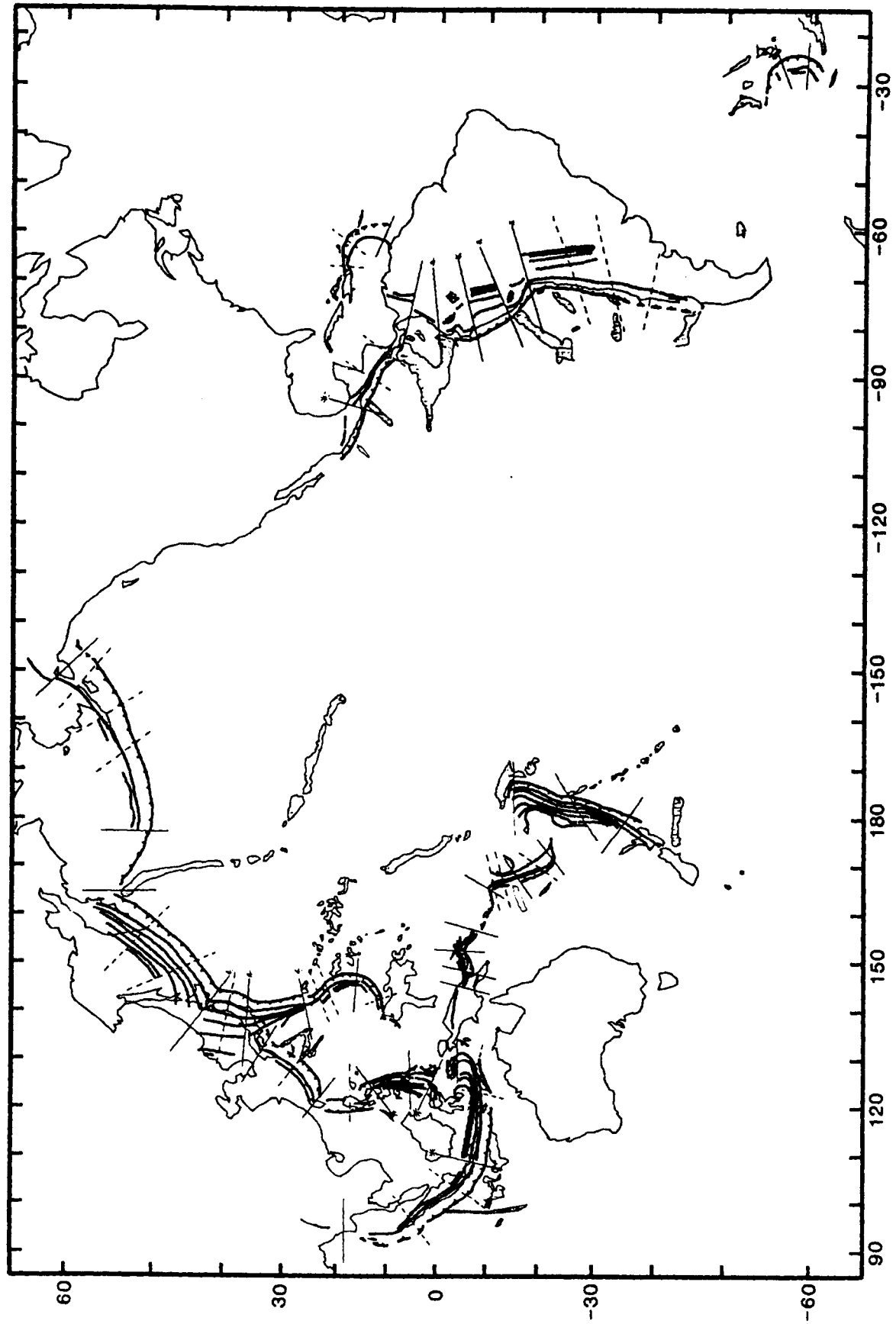

Fig. 2. Contours of the mean depth of seismicity for the Wadati-Benioff zones of the circum-Pacific. Contour interval is 100 km. Dashed contours are inferred where there is not enough seismicity to define the contour directly. Lines perpendicular to the contours are PSBs delineated in this study. Dashed PSBs are poorly defined; solid PSBs are well constrained; and asterisks indicate the best defined PSBs. Shaded regions represent bathymetric features that are interacting with subduction zones.

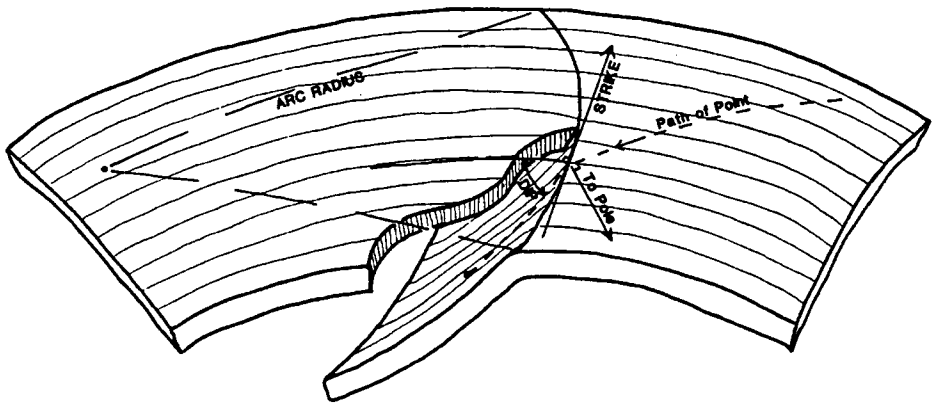

Fig. 3. Schematic of the ideal subduction geometry showing how the modeling of subduction geometries was accomplished (see text).

we organize the mechanisms into groups of events with similar locations and/or similar mechanisms.

Analysis of Wadati-Benioff Zone Structure and Possible Segment Boundaries

Using software developed by *Bennett* [1985] on an Evans and Sutherland PS-300 graphics system, we can project a group of hypocenters into a three-dimensional image on a screen and view them from any angle simply by turning dials. This technique allowed very thorough and efficient examination of the Wadati-Benioff zone structure without the distortion or the inherent subjectivity of two-dimensional cross sections.

We use this graphics system in conjunction with maps and cross sections of hypocenters to delineate Wadati-Benioff zone structures, and record the structures as contours on a map (Figure 2). In this study, the mapped contours represent the mean depth of seismic activity, rather than the upper surface of the plate. In the figures, dashed contours are structures that were less certain than others.

While examining the ISC-*pP* data in this way, we searched for any abrupt changes in the seismicity or structure along the strike of the Wadati-Benioff zones. In order to be as objective as possible, we compiled a list of characteristics that might indicate the presence of such a change (Table 1). Wherever one or more of these characteristics occurs, we drew a line defining a PSB (Figure 2 and Table 2). Each PSB was labeled as either "well constrained" or "poorly constrained" on the basis of the number and quality of the characteristics associated with it. In the figures, all well-constrained PSBs appear as solid lines, and all poorly constrained PSBs as dashed lines (Figure 2 and Figures 9-20). The best constrained PSBs are labeled with asterisks.

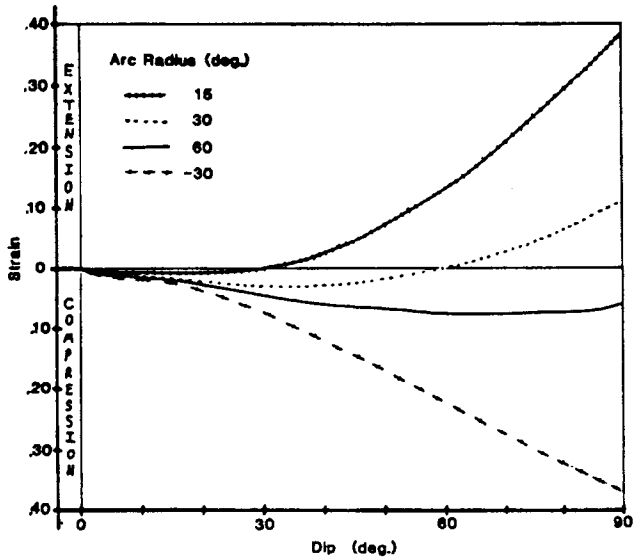

Fig. 4. Lateral strain versus dip for various arc radii. In each case the strain is for 10° of orthogonal subduction about a pole 90° away from the center of the arc. These results are consistent with theoretical results determined analytically based on subduction of a thin spherical shell (the ping-pong ball model).

Definition of Terms

In this study, the terms "PSB", "boundary", and "segment boundary" refer to specific transverse features of the Wadati-Benioff zone or of the subducted plate. None of these terms carry any implicit connotation about the physical nature of the feature, or about its tectonic significance. The term PSB refers only to the possible segment boundaries delineated in this study as described above. The term segment will denote the portion of subducted lithosphere between two adjacent PSBs, or between specific boundaries proposed by other investigators. This term also carries no implication as to the physical nature of the boundaries.

We use the terms "tear" and "contortion" to discuss the physical nature and/or tectonic significance of various

TABLE 1. Characteristics Used to Delineate Possible Segment Boundaries's

	Percent of Possible Segment Boundaries	
	Characteristics	All
Abrupt change in strike of Wadati-Benioff zone	41	66
Abrupt change in dip of Wadati-Benioff zone	45	72
Offset of Wadati-Benioff zone	35	49
Abrupt change in the maximum depth of seismicity	70	80
Gap in seismicity (deep, intermediate, or shallow)	49	55
Cluster or lineation of earthquakes	4	6
Abrupt end of Wadati-Benioff zone	19	30

The percentages of all PSBs and well constrained PSBs which showed each characteristic are recorded to the right. Well constrained, both here and in the text, refers to PSBs with at least one "A"-graded characteristic, or at least two "B"-graded characteristics. All others were considered "poorly constrained." See Table 2.

TABLE 2. Characteristics

	Quality of Possible Segment Boundaries	Strength of Characteristics†						
		I	II	III	IV	V	VI	VII
South America								
SA1	good		fair	fair	strong	fair		
SA2	good*		strong	strong	fair	strong		
SA3	good*		strong	strong	fair	strong		
SA4	good*		strong	strong	fair	strong		
SA5	good*		strong	strong	fair	strong		
SA6	poor	fair				weak		
SA7	poor			weak		fair		
SA8	poor	weak						weak
Middle America								
MA1	good*	strong	strong	strong	fair	strong		
MA2	poor		weak	weak				
MA3	poor					weak		weak
Eastern Caribbean								
EC1	poor	weak	weak	weak	fair			
EC2	poor	fair	weak					
EC3	good	strong	fair					
South Sandwich								
SS1	good*	fair	strong	strong	strong	fair		
SS2	good		strong			fair		

of Possible Segment Boundaries

Other Phenomena Correlated with Possible Segment Boundaries							
Change in Trench Morphology	Strength of Correlation	Bathymetric Ridges	Strength of Correlation	Change in Volcanism	Strength of Correlation	Focal Mechanisms	Strength of Correlation
				end of volcanic line	strong		
change in depth or break in trench	fair	ridge at possible segment boundaries (PSBs)	strong	cluster	fair		
		ridge to one side of possible segment boundary (PSB)	fair				
change in depth or break	fair	ridge to one side of PSB	strong				
change in strike or trench	strong	ridge to one side of PSB	strong	offset or change in lineation	fair	anomalous	fair
		ridge to one side of PSB	weak	end of volcanic line	fair		
		ridge at PSB	strong	end of volcanic line	strong	anomalous	weak
		ridge to one side of PSB	weak				
change in depth or break in trench	fair	ridge at PSB	strong	change in strike, depth or break in trench	strong	anomalous	fair
		ridge to one side of PSB	fair				
change in depth or break in trench	strong	ridge to one side of PSB	strong	offset or change in lineation	fair	hinge faulting	strong
		ridge at PSB	fair				
change in strike of trench	fair	ridge to one side of PSB	fair	end of volcanic line	fair		
				end of volcanic line	strong		
		ridge to one side of PSB	fair	offset or change in lineation	fair	anomalous	fair
		ridge to one side of PSB	fair	offset or change in lineation	fair		

TABLE 2.

	Quality of Possible Segment Boundaries	Strength of Characteristics†						
		I	II	III	IV	V	VI	VII
Alaska-Aleutian								
AA1	good	weak	fair	fair	fair			
AA2	poor	weak	fair	weak				
AA3	poor	weak				fair		
AA4	poor	fair						
AA5	good		weak			strong		
AK	good						strong	
Kurile-Kamchatka								
KK1	poor					fair		
KK2	poor					fair		
Japan								
HOK	good*	strong	strong	strong		fair		
JAP	poor	fair						
Izu-Bonin								
JIB	good*	strong	strong	strong	fair	fair		
IBM	good*	strong	strong	strong	strong	fair		
Mariana								
M1	good	fair			fair	weak		
M2	good	fair			fair	weak		
M3	good	strong	strong	fair		strong		
M4	poor	weak	fair		weak			
Ryuku								
RY1	good		strong			strong		strong

(continued)

Other Phenomena Correlated with Possible Segment Boundaries							
Change in Trench Morphology	Strength of Correlation	Bathymetric Ridges	Strength of Correlation	Change in Volcanism	Strength of Correlation	Focal Mechanisms	Strength of Correlation
change in strike of trench	weak			end of volcanic line	strong		
change in strike of trench	weak			offset or change in lineation; change in number or character	strong		
change in strike of trench	fair			end of volcanic line	fair		
change in strike of trench	strong	ridge at PSB	strong				
		ridge to one side of PSB	weak	offset or change in lineation	strong		
change in strike of trench				offset or change in lineation			
change in strike of trench	strong			offset or change in lineation	strong	hinge faulting	fair
change in strike of trench	strong	ridge at PSB	strong	offset or change in lineation	weak faulting	hinge	weak
				offset or change in lineation	fair		
		ridge to one side of PSB	fair	cluster	fair		
change in strike of trench	fair	ridge to one side of PSB	fair				
change in strike of trench	weak	ridge at, and to one side of PSB	fair				
change in strike, and depth or break in trench	strong	ridge at PSB	weak	end of volcanic line	strong		

TABLE 2.

	Quality of Possible Segment Boundaries	Strength of Characteristics†						
		I	II	III	IV	V	VI	VII
RY2	poor					fair		
RY3	good		strong	fair		strong	strong	fair
MAN	weak		fair	weak				
Philippines								
PH1	good*	fair	fair	strong	strong	strong		strong
PH2	good			strong	strong			
PH3	good*	fair	strong	strong	strong	strong		
Java								
JV1	good	strong						strong
JV2	poor		weak			fair		
JV3	poor	weak				fair		
JV4	good*	fair	fair	fair	weak	strong		
JV5	poor	fair	weak	weak				
JV6	poor	fair	weak	weak				
JV7	good	fair	fair	fair		fair		

(continued)

Other Phenomena Correlated with Possible Segment Boundaries							
Change in Trench Morphology	Strength of Correlation	Bathymetric Ridges	Strength of Correlation	Change in Volcanism	Strength of Correlation	Focal Mechanisms	Strength of Correlation
change in depth or break in trench	strong			end of volcanic line	fair		
change in strike, and depth or break in trench	strong			change in number or character; cluster	strong faulting	hinge	fair
change in strike of trench	strong			offset or change in lineation	strong	anomalous	fair
change in strike of trench	weak			offset or change in lineation; change in number or character	fair	anomalous; hinge faulting	weak
change in strike and in depth or break of trench	strong			change in number or character	weak		
				end of volcanic line	strong faulting	anomalous; hinge	fair
change in depth or break in trench	strong			end of volcanic line	strong		
change in strike of trench	strong			end of volcanic line	strong		
change in strike of trench	fair	ridge at PSB	weak				
change in strike of trench	weak	ridge at PSB	weak	offset or change in lineation; cluster	weak		
change in depth or break in trench	strong			change in number or character; cluster	strong		
change in strike and in depth or break in trench	strong			change in number or character; cluster	strong		
change in strike and in depth or break in trench	strong			end of volcanic line	strong		

TABLE 2.

	Quality of Possible Segment Boundaries	Strength of Characteristics†						
		I	II	III	IV	V	VI	VII
Tonga-Kermadec								
TK1	good							strong
TK2	good	fair		fair		fair		
TK3	good	strong		fair		strong		
New Hebrides								
NH1	poor					fair		
NH2	poor					fair		
NH3	good	strong			fair	strong		
NH4	poor	weak				fair		
NH5	good		strong	fair		strong		strong
New Britain								
NB1	good							strong
NB2	good	strong	strong	fair	fair	fair		
NB3	good		weak	strong		strong	fair	
NB4	good	weak	weak	strong	strong	strong		
NB5	good							strong

* Indicates best 12 possible segment boundaries.

† Characteristics used to delineate possible segment boundaries. (See also Table 1.) I., Abrupt change in strike of Wadati-Benioff zone; II., Abrupt change in dip of Wadati-Benioff zone; III., Offset of Wadati-Benioff zone; IV., Abrupt change in the maximum depth of seismicity; V., Gap in seismicity (deep, intermediate, or shallow); VI., Cluster or lineation of earthquakes; VII., Abrupt end of Wadati-Benioff zone.

(continued)

Other Phenomena Correlated with Possible Segment Boundaries							
Change in Trench Morphology	Strength of Correlation	Bathymetric Ridges	Strength of Correlation	Change in Volcanism	Strength of Correlation	Focal Mechanisms	Strength of Correlation
change in strike of trench	strong	ridge at PSB	strong	offset or change in lineation; change in number or character	weak faulting	hinge	strong
change in strike of trench	strong	ridge at PSB	strong			anomalous	strong
				change in number or character	fair	anomalous	fair
						hinge faulting	weak
		ridge to one side of PSB	fair	end of volcanic line	fair	hinge faulting	weak
change in depth or break in trench	strong	ridge at PSB	strong			anomalous	strong
				offset or change in lineation; change in number or character	fair	anomalous	fair
change in strike of trench	strong			end of volcanic line	strong faulting	hinge	fair
change in depth or break in trench	strong			offset or change in lineation; cluster	strong		
change in strike of trench	strong			offset or change in lineation; change in number or character	strong	anomalous	fair
change in depth or break in trench	fair			cluster	fair	anomalous	fair
change in depth or break in trench	strong			change in number or character; cluster	fair	anomalous; hinge faulting	fair

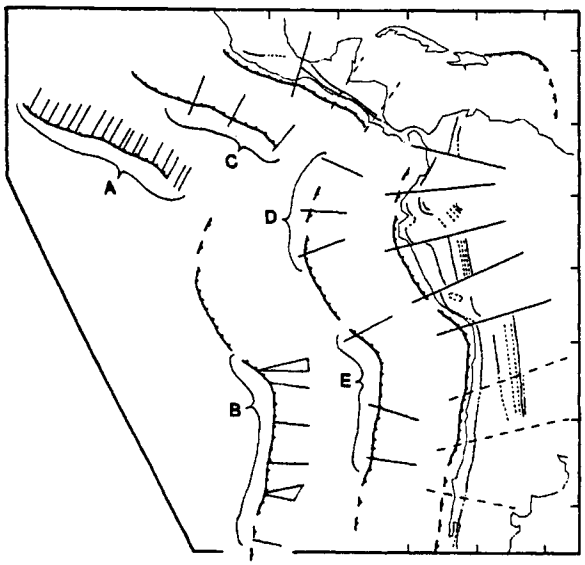

Fig. 5. Comparison of the results of this study with segmentation proposed by previous authors: A, *Stoiber and Carr* [1973]; B, *Swift and Carr* [1974]; C, *Burbach et al.* [1984]; D, *Pennington* [1981]; and E, *Barazangi and Isacks* [1976, 1979*a*, *b*].

boundaries. We use the term tear to describe a discontinuity, usually a hinge fault, representing a brittle deformation of the subducting plate such that the segments on either side can move independently. We use the term contortion to describe a ductile deformation of the subducting plate such that the plate remains coherent across the boundary.

Modeling Subduction Geometries and Lateral Strain

To estimate the amount of lateral strain represented by the observed subduction geometries, we developed a simple method of modeling subducted plates (see the appendix). Beginning with a digitized representation of the trench geometry, we subduct each point along the trench in a manner depending on the pole of rotation for the two plates, the local dip of the Wadati-Benioff zone, and the local strike of the trench (Figure 3). Each point is subducted independently of adjacent points by an amount equivalent to 10 Ma of rotation.

We use the change in distance between adjacent points before and after subduction to define the lateral strain. Note that this strain is not necessarily the maximum strain, nor the horizontal strain; rather it is the strain along the 10-Ma isochron connecting points subducted simultaneously. To test the modeling method, we determined the lateral strain for various hypothetical subduction geometries having constant arc radii and dips (Figures 3 and 4).

We have applied this modeling technique to the major subduction zones of the circum-Pacific area. In a few regions where the Wadati-Benioff zone structure was complicated, we chose models which simplified the observed structure. In a few other regions, such as the New Britain-New Guinea area, the structure is too complex to model adequately with this method.

The maps and cross sections (Figures 9-20) present the results of the modeling, showing the paths of the individual points as they were subducted, and the location of those points at 5 Ma and 10 Ma. In some cases the Wadati-Benioff zone extends beyond the 10-Ma line, and in other cases the 10-Ma line extends well beyond the extent of the Wadati-Benioff zone. In some regions, such as South America, this discrepancy occurs because the deep earthquakes are not situated on the direct extension of the structure defined by the uppermost 300 km of the Wadati-Benioff zone. In most cases the 10-Ma line coincides with the extent of the Wadati-Benioff zone.

DISCUSSION AND CONCLUSIONS

Limitations of the Data

The teleseismic data used in this study (ISC-*pP* data, Figure 1) adequately define the major features of most Wadati-Benioff zones, but these data do have some limitations. Most important is the limit of resolution due to scatter and heterogeneous distribution of the data. In regions where events are plentiful and the structure is regular, the ISC-*pP* data indicate apparent Wadati-Benioff zone thicknesses of 30-40 km. It is unclear how much of this thickness is real and how

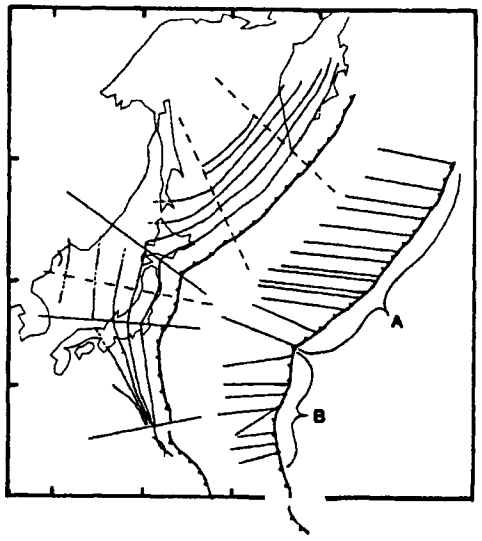

Fig. 6. Comparison of the results of this study with segmentation proposed by previous authors: A, *Veith* [1974]; and B, *Carr et al.* [1973].

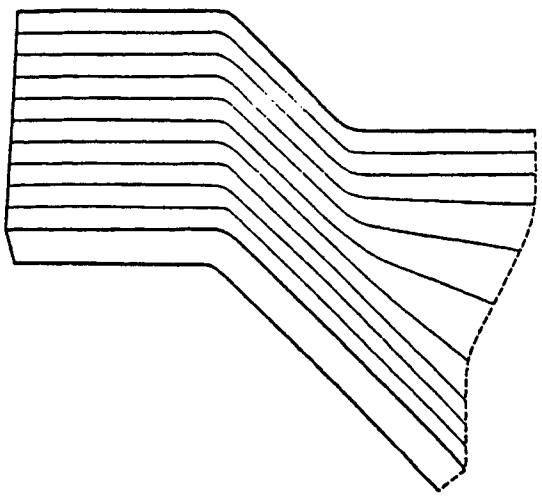

Fig. 7. Schematic representation of the structure of the subducted plate beneath southern Peru as determined from local microearthquake studies [from *Hasegawa and Sacks*, 1981].

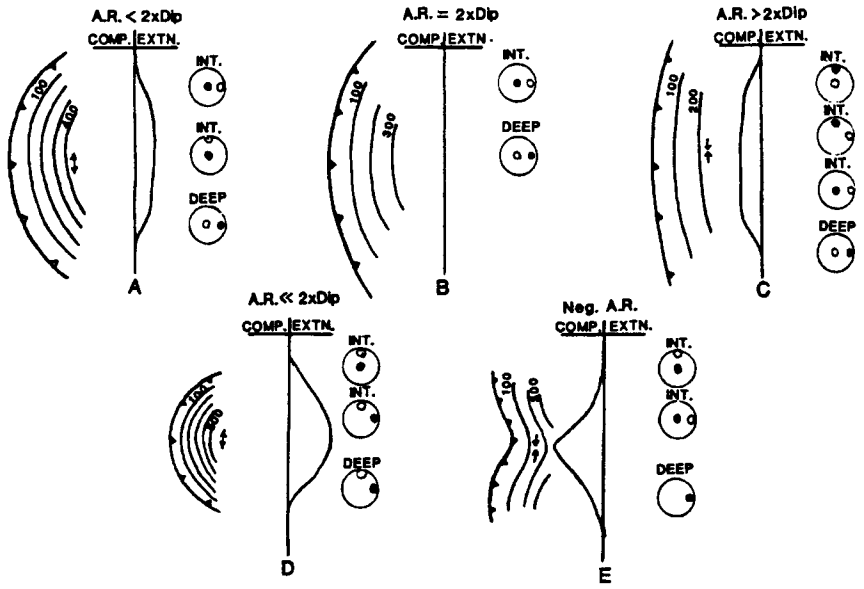

Fig. 8. Generalizations about the relationships of subduction geometry, lateral strain, and intermediate and deep focal mechanisms. Each figure includes a model showing a trench and contours of the subducted plate, a graph showing lateral strain along the arc, and representative intermediate and deep focal mechanisms. The focal mechanisms are lower hemisphere projections with P axes shown as solid circles and T axes shown as open circles. Double arrows indicate the directions of the lateral strains.

much is due to scatter in the data, but this does provide a minimum estimate of the resolution of the data. In regions where the data are well distributed, we should be able to delineate any change in structure that produces more than 30-40 km of relief in the Wadati-Benioff zone. In regions where the data are sparse or distributed unevenly, or where a change in structure is associated with a marked decrease in seismicity, the resolution is greatly reduced.

Because the ISC catalog contains many poorly located events which would greatly increase the scatter in the data, using the complete ISC catalog would not increase the resolution. As shown by *Stark and Frohlich* [1985] for deep events, most earthquakes with depths constrained by *pP-P* intervals have body-wave magnitudes of 5.0 or greater, and so are likely to be more accurately located than smaller events reported by the ISC.

Local network data usually have better resolution than the ISC-*pP* data, but local networks cover only a small fraction of the Wadati-Benioff zones observable teleseismically. Also, local networks near subduction zones often suffer from systematic location problems that do not affect teleseismic data [*Barazangi and Isacks*, 1979*b*; *McLaren and Frohlich*, 1985]. Comparison of the results of this study with published results from local network data (as will be discussed later) suggests that the ISC-*pP* data are surprisingly good for providing a faithful picture of Wadati-Benioff zone structure.

The historical data for the years 1900-1963 also suggest that the ISC-*pP* data adequately represent the distribution of intermediate and deep seismicity. Although few of the historical earthquakes are well enough located to be helpful in delineating details of Wadati-Benioff zone structures, they do show the gross distribution of the seismicity. Only in a single case, that of the Spanish deep earthquake of March 29, 1954 [*Udias et al.*, 1976], do the historical data indicate deep seismicity where the ISC-*pP* data do not. While there are also two deep historical earthquakes beneath Colombia which are fairly distant from most other deep activity, they are less than 200 km from the Colombian deep earthquake of July 31, 1970 [*Furumoto*, 1977], which is included in the ISC-*pP* data. Finally, there are a few intermediate-depth historical earthquakes near Japan and the Kurile Arc that are significantly out of place with respect to the structure observed in the ISC-*pP* data, but these events are probably mislocated. There are other regions where intermediate or deep events have been reported, but are probably mislocated [*Asudeh*, 1983; *Dzhibladze*, 1983].

There are also two regions where there is known intermediate-depth activity that does not show up in the ISC-*pP* data. Microseismic studies indicate a zone of intermediate-depth events beneath the Fiordland region of South Island, New Zealand [*Smith and Davey*, 1984]. While a few of these events were located teleseismically and reported by the ISC, none have depths constrained by *pP-P* intervals. A few deep events have also been reported beneath North Island, New Zealand, farther south than any deep events in the ISC-*pP* data [*Adams and Ferris*, 1976]. Similarly, the Mediterranean subduction zones [*Bottari and Neri*, 1983; *Makropoulos and Burton*, 1984] show up only as a few isolated intermediate-depth events in the ISC-*pP* data.

Thus, in spite of its limitations, the ISC-*pP* data set is the best available for a global study of Wadati-Benioff zone structure. It provides adequate coverage, both in time and in space, with good resolution for most major subduction zones. Although in some regions other data can increase the resolution or provide supporting evidence for lateral changes in structure, we know of no case where either local network data, volcanism, or historical seismic data indicate a major change in structure that is not observable in the ISC-*pP* data.

Segmentation

Where are the segment boundaries? The answer to this question depends largely on the definition of terms, as discussed earlier. The most straightforward answer is that the

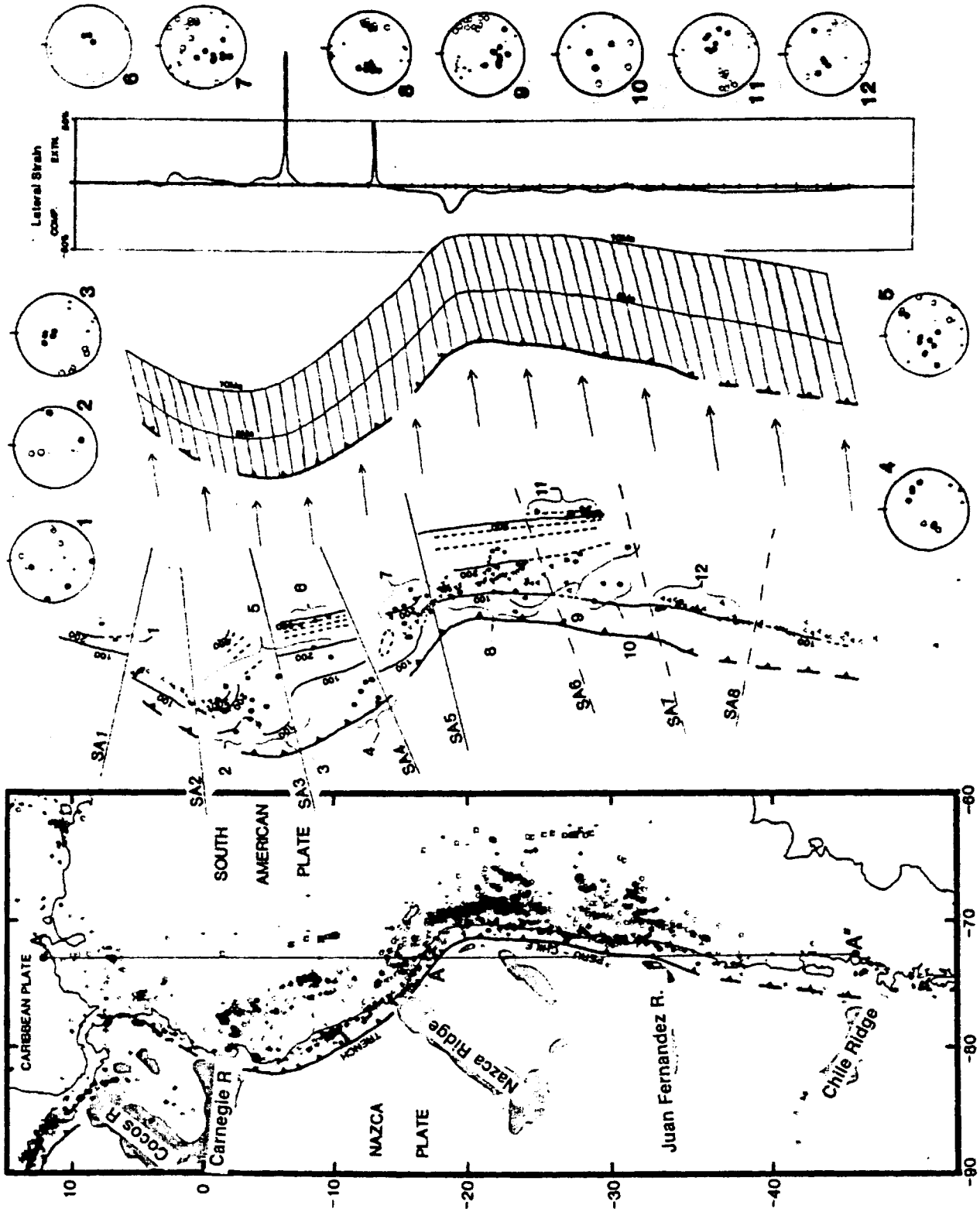

Fig. 9. Results of this study for South America.

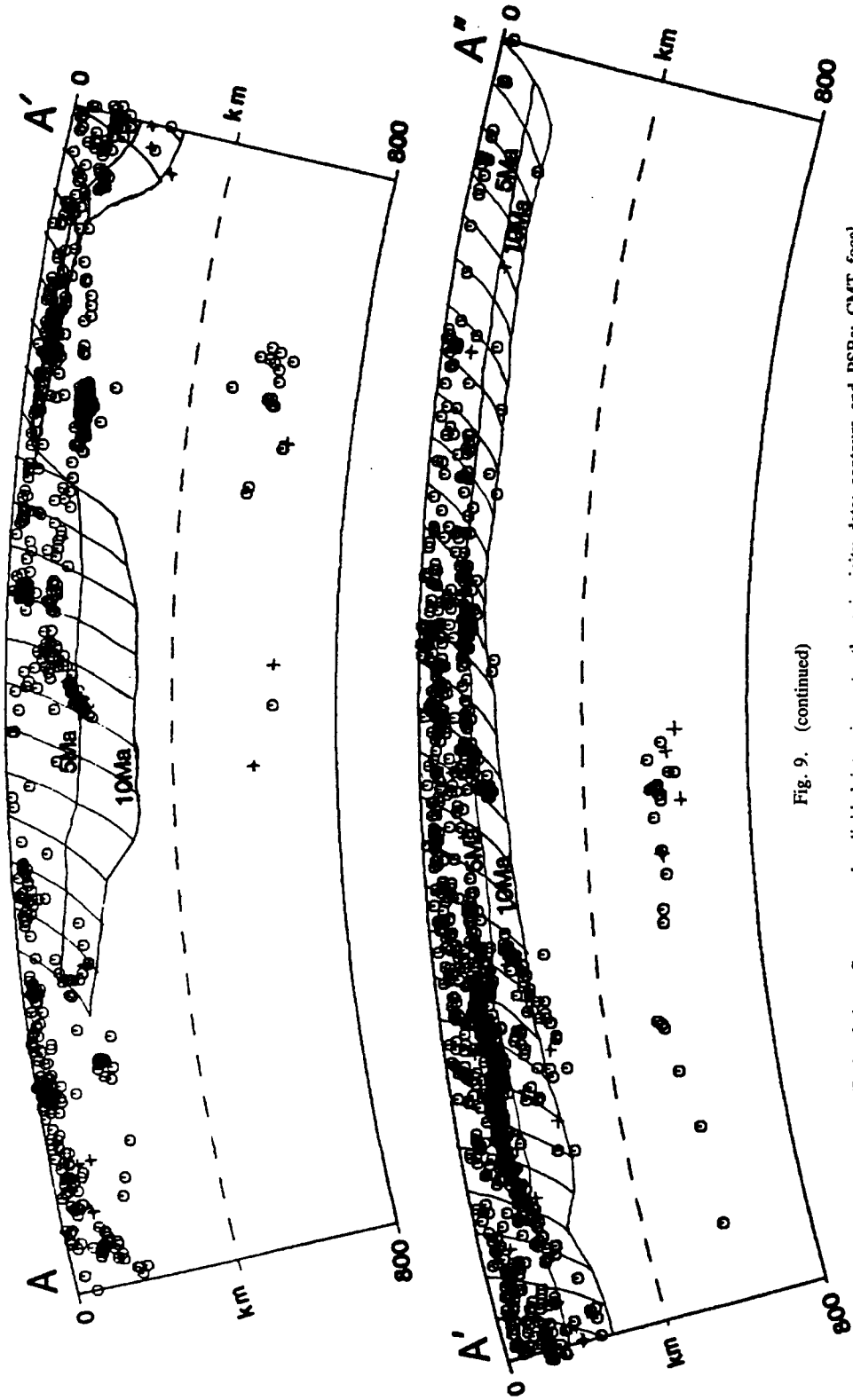

Fig. 9. (continued)

Figures 9-20. Each of these figures can be divided into six parts: the seismicity data; contours and PSBs; CMT focal mechanisms; modeled geometry; lateral strain; and lateral cross sections. For the seismicity data, open symbols are ISC-*pP* epicenters as follows: diamonds, 0-70 km; circles, 70-300 km; and squares, >300 km. The crosses are epicenters of historical earthquakes. The contours represent the mean depth to the Wadati-Benioff zone in 100-km intervals. Dashed contours are inferred where there was not sufficient data to delineate them directly. Open triangles represent active volcanoes. Solid PSBs are well constrained and dashed PSBs are poorly constrained. Solid dots indicate epicenters of events for which there are CMT mechanisms, and the numbered groupings correspond to the numbered focal mechanisms. The CMT mechanisms are lower-hemisphere projections with symbols as follows: Solid circles, *P* axes; open circles, *T* axes; and crosses, *N* axes. For the models the lines perpendicular to the trench represent the surface projections of the paths followed by points as they are subducted; the lines parallel to the trenches indicate the positions of the points after 5 and 10 Ma (million years) of subduction. The modeled geometries are also shown in the cross sections. The arrows are convergence vectors with lengths equal to 5 Ma of motion. The graphs show lateral strain after 10 Ma predicted from the model, and are lined up with the points at the 10-Ma line. The cross section locations are indicated on the map with the seismicity data. On the cross sections, all ISC-*pP* events are open circles and the historical events are crosses. On the deep cross sections the dashed line represents the 400-km level.

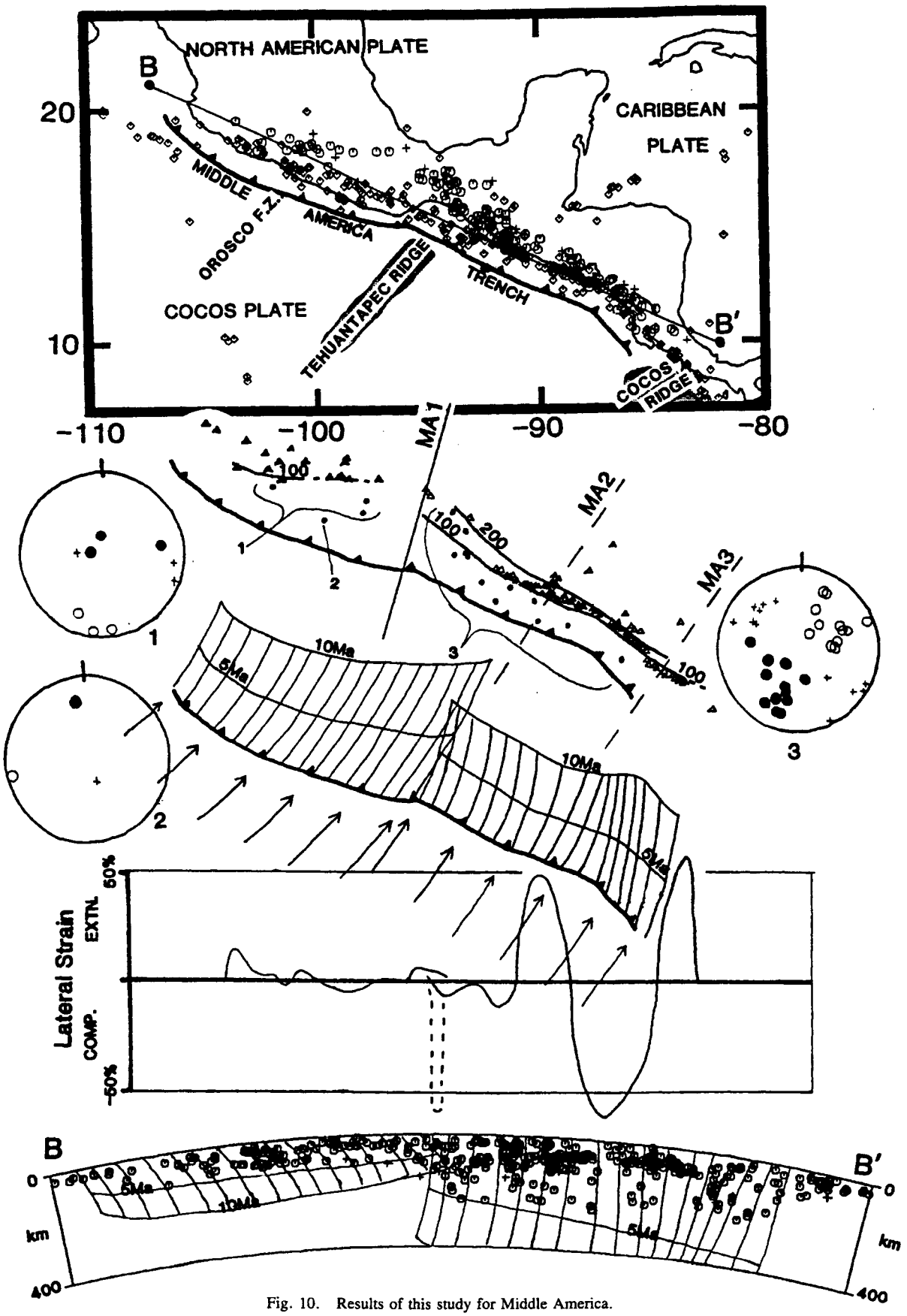

Fig. 10. Results of this study for Middle America.

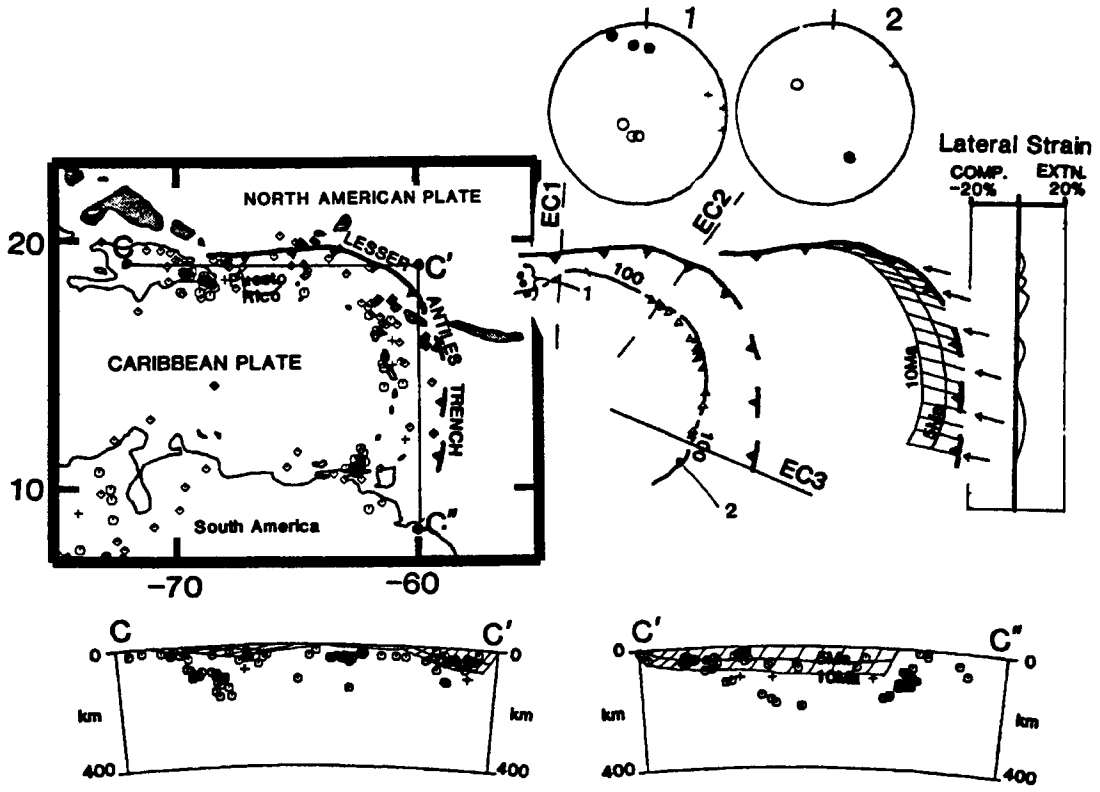

Fig. 11. Results of this study for the eastern Caribbean.

boundaries are the PSBs of Figure 2 and Table 2, with some boundaries being of higher assessed quality than others. These 57 PSBs represent every significant change in seismicity or structure visible in the ISC-*pP* data. Some of the poorly constrained PSBs were delineated on the basis of weak changes in only one or two characteristics, and may be artifacts of inadequate sampling and/or heterogeneous distribution of the seismicity. Thus, a few of these PSBs may have no tectonic significance. Many of the PSBs, however, were very well constrained, involving abrupt changes in structure and seismicity. The 12 best PSBs, marked with asterisks in Figure 2 and Table 2, all possessed at least four of the first five characteristics in Table 1.

Other investigators have used different data and criteria to determine segment boundaries. *Stoiber and Carr* [1973] delineated segment boundaries on the basis of discontinuities in the volcanic line. Others have used changes in shallow focal mechanisms [*Dean and Drake*, 1973], the extent of rupture planes of great earthquakes [*Swift and Carr*, 1974; *Frankel and McCann*, 1979], or changes in the bathymetry along the trench [*Spence*, 1977]. However, most investigators have also used either teleseismic or local seismicity data to delineate changes in the Wadati-Benioff zone structure. These differences in approach, and differences in investigators' presuppositions about segmentation, have led to very different interpretations in some regions (Figures 5 and 6).

Several investigators have used local network data to delineate segment boundaries. All of these boundaries correspond to PSBs delineated in this study, but the local network data generally provides significantly more detail than the ISC-*pP* data. For example, the PSB beneath Cook Inlet, Alaska (AA2 in Figure 13), is very poorly defined in the ISC-*pP* data, and could easily have been missed, or explained as an artifact of poor distribution of the data, but the local network data of *Pulpan and Frohlich* [1985] show that this PSB does represent a real change in structure. Similarly, the local network data of *Matumoto et al.* [1976] and *Liaw* [1982] help substantiate a poorly defined PSB beneath Costa Rica (MA3 in Figure 10). In the Puerto Rico region, *McCann and Sykes* [1984] used local network data to delineate a tear that corresponds to EC1 (Figure 11), suggesting that that is indeed a significant boundary, but the fact that they did not delineate a segment boundary in the vicinity of EC2 suggests that EC2 may be an artifact of poor distribution of the data.

Even for well-defined PSBs, local network data often improve the resolution of the structure. Beneath southern Peru, *Hasegawa and Sacks* [1981] and *Grange et al.* [1984*a*, *b*] used local network data to show that the boundary proposed by *Barazangi and Isacks* [1976, 1979*a*] was actually a broad contortion of the subducting plate, rather than a tear (Figure 5). This contortion is located between two of the most reliable PSBs from this study (SA4 and SA5 in Figure 9). A major limitation of relying on local network data alone to delineate PSBs is that such networks cover only a very small portion of the teleseismically observable Wadati-Benioff zones.

Changes in the locations or types of volcanoes have also been used to delineate segment boundaries [*Stoiber and Carr*, 1973; *Carr et al.*, 1979]. Active volcanoes usually occur above the 70- to 200-km-deep portion of the Wadati-Benioff zone beneath most arcs. About 68% of all the PSBs delineated in this study (including 10 of the best 12) are associated with some noticeable change in arc volcanism. Unfortunately, the PSBs and changes in volcanism seldom coincide exactly and are often separated by as much as 100 km. Indeed, in many cases it is not clear whether an observed PSB and change in volcanism are related.

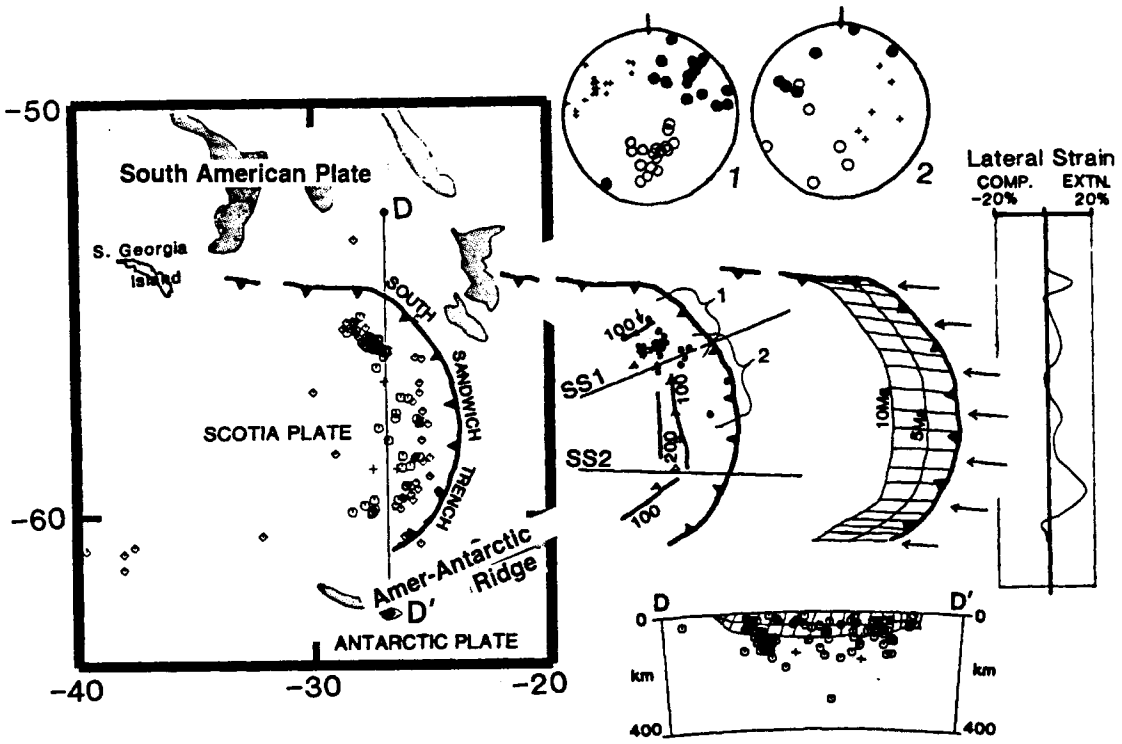

Fig. 12. Results of this study for the South Sandwich Arc.

A particularly interesting example is the abrupt end of the volcanic line in southern Peru. This change in volcanism lies almost midway between two extremely well-constrained PSBs (SA4 and SA5 in Figure 9), but not close enough to clearly associate it with either. This change in volcanism coincides with the segment boundary proposed by *Barazangi and Isacks* [1976, 1979*a*]. In this case the change in volcanism may indicate a segment boundary that wasn't visible in the ISC-*pP* data. However, it is also possible that the change in volcanism is related to the broad change in structure across both the observed PSBs, rather than to a single segment boundary.

Changes in volcanism help substantiate the tectonic significance of PSBs, but there are some problems with using these changes to delineate segment boundaries directly. The exact physical processes that cause volcanism to occur above subducting plates is unknown, and the volcanic line is separated from the subducting plate by 70-200 km of mantle and crust. The structure of the overriding plate may influence the exact locations of the volcanoes at least as strongly as the structure of the subducting plate [*Nixon*, 1982]. This influence is evident at the western end of the volcanic chain in Central America (Figure 10). There is no PSB at this location, but it is very near a major triple junction. It is likely that the termination of the volcanic chain is related to the boundary between the two overriding plates, the North American and Caribbean plates, rather than to segmentation of the subducting plate [*Burbach et al.*, 1984].

What is the mode of deformation? Are most segment boundaries tears or ductile contortions of the subducting lithosphere? Most investigators have interpreted their segment boundaries as tears, but we believe that few of the PSBs delineated in this study are actual tears. There is ample evidence of abrupt changes in structure in the teleseismic data, but very little evidence of hinge faulting, overlapping segments, or other clear indications that the PSBs are actually tears.

Most of the 12 best constrained PSBs exhibit changes in the strike, dip, and maximum depth of seismicity that are quite abrupt. In some regions, such as the Hokkaido corner and the Japan/Izu-Bonin corner, the data can easily fit a structure that is continuous across the PSBs, at least to intermediate depths. In other regions, such as in northern South America, it was difficult to draw continuous structures across the PSBs, and it was tempting to interpret these PSBs as tears.

In substantial agreement with the present study, *Yamaoka et al.* [1986] found that the geometry of most observed subduction zones could be fit by deformation of inextensible vinyl shells without tearing. They found tears necessary in only five places: the South Sandwich Arc, the southern Mariana Arc, the northern Tonga Arc, the southern Ryukyu Arc, and the Banda Sea region. In addition, they noted possible tears in the Peru-Chile and New Hebrides regions. These proposed tears correspond very well to PSBs SS1, M3, TK1, RY3, JV6, SA5, and NH3, all of which are well defined except JV6.

Isacks and Barazangi [1977] reviewed the problem of lateral segmentation in the upper 300 km of subducted plates and concluded that the only place where a tear was well constrained was beneath southern Peru. Nevertheless, several investigations using local network data have convincingly shown that the subducted plate in this region (Figure 7) is not torn, but sharply contorted [*Hasegawa and Sacks*, 1981; *Schneider*, 1984; *Grange et al.*, 1984*a*, *b*]. This contortion occurs in the vicinity of two of the best constrained PSBs (SA4 and SA5 in Figure 9). Of all the PSBs delineated in this study, these PSBs are the two for which discontinuous structures seemed to fit the data best. If the subducted

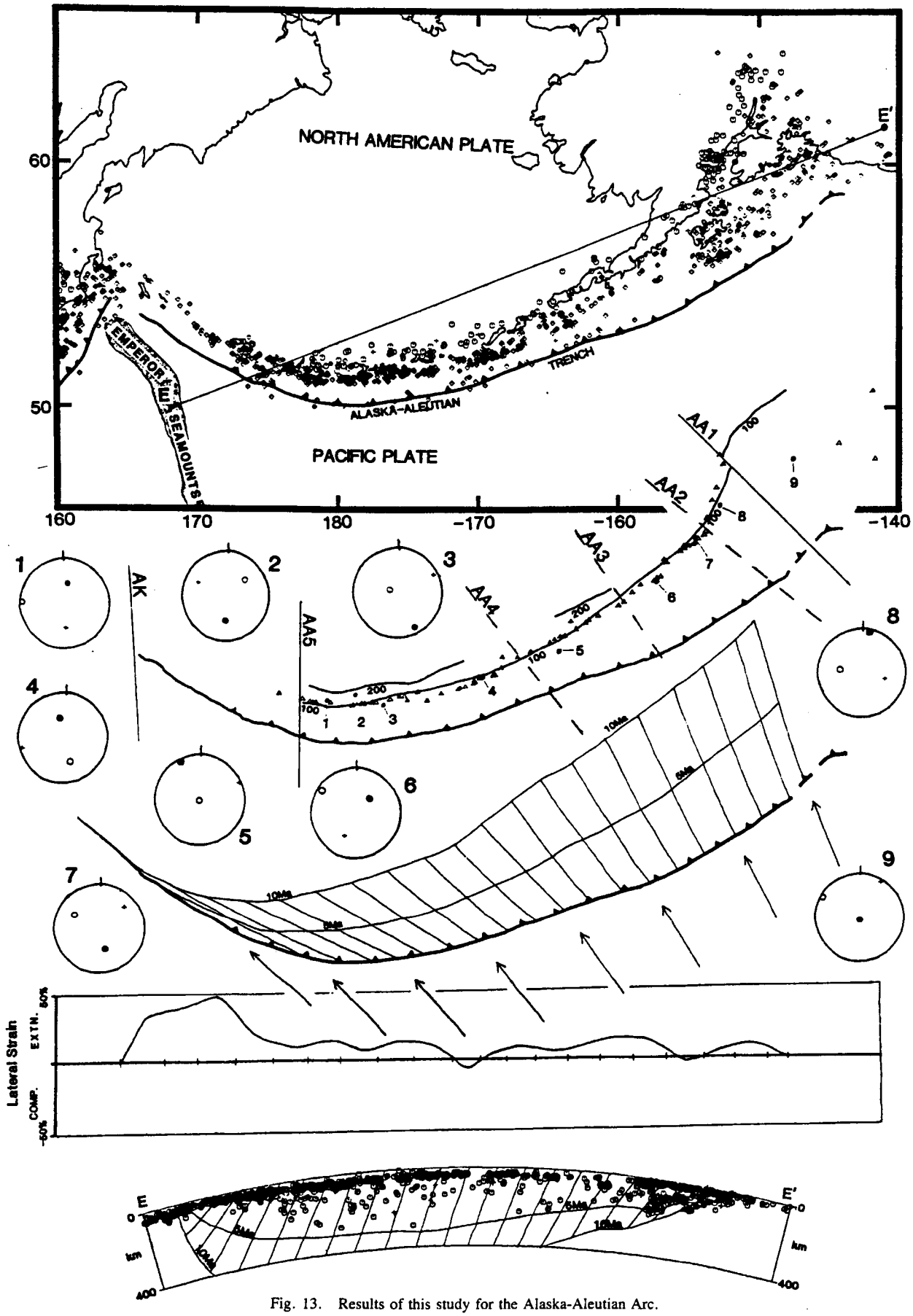

Fig. 13. Results of this study for the Alaska-Aleutian Arc.

lithosphere in the region of these PSBs has deformed ductilely rather than by tearing, it seems reasonable to expect that ductile deformation occurs at most other PSBs.

Tears have been proposed on the basis of local network data for other regions, such as Costa Rica [*Matumoto et al.*, 1976; *Liaw*, 1982], and Cook Inlet, Alaska [*Pulpan and Frohlich*, 1985], but the evidence for these proposed tears is not nearly as conclusive as the evidence against a tear in southern Peru. These proposed tears are associated with PSBs that are only poorly defined in the ISC-*pP* data. The local network data of *Pulpan and Frohlich* [1985] indicate a small amount of apparent overlap between the two segments on either side of their boundary. In other places this overlap would provide strong support for the presence of a tear. In this case, however, both the trench and the Wadati-Benioff zone form a convex seaward bend. If there was a tear, this geometry would require the opening of a gap between the segments, not an overlap. The meaning of this apparent overlap is not clear.

One might expect to find tears where there are abrupt changes in the geometry of the trench. Perhaps the most drastic changes in trench geometry occur at the Hokkaido corner and at the Japan/Izu-Bonin corner (Figure 14). In both regions, the geometry is such that, if there were a tear, the two segments would have to overlap. In both of these regions the seismicity fits a continuous but contorted structure down to at least 300 km, and there is no sign of any overlap. Below 300 km there is a notable absence of seismic activity at both corners. As shown by *Aoki* [1974], there is a possible small tear at the Japan/Izu-Bonin corner below about 200 km, but it is not clear. *Kanamori* [1971] suggested that there might be a tear beneath the Hokkaido corner, but that the lateral compression across the corner kept the two edges together, resulting in the observed buckling.

One might expect a tear separating independently subducting blocks of lithosphere to be seismically active, exhibiting lineations or increases in seismicity. Most PSBs, however, are associated with gaps or lower levels of seismic activity. One could explain this if the two sides of the tear were free edges of descending plates that are completely uncoupled past the point where the tear originates. This explanation would be plausible for tears in regions under lateral extension, but not in regions of lateral compression. Most of the best constrained PSBs occur in regions which the modeling predicts to be under lateral compression.

If a tear separates blocks subducting at different dips, focal mechanisms might show evidence of hinge faulting. The best evidence of hinge faulting in the CMT mechanisms occurs in regions where a trench ends at a transform boundary such that lithosphere on one side of the transform is subducted, while that on the other side is not. This situation occurs at the southern end of the New Hebrides Trench (Figure 19), and at the northern ends of the Tonga and South Sandwich Trenches (Figures 18 and 12, respectively). There is also evidence of hinge-faulting in regions where there is a reversal of polarity along a subduction zone, such as near Taiwan (Figure 18), possibly in the northern Philippines (Figure 18), and in eastern New Guinea (Figure 20).

The fact that hinge faulting events do occur where tears are geometrically required suggests that hinge faulting events should also accompany tears within otherwise continuous subducting slabs. There are a few anomalous mechanisms in other regions that may indicate hinge faulting, but they are not clear enough to provide conclusive evidence for tears. These regions include the Japan/Izu-Bonin and Izu-Bonin/Marianas junctions and two PSBs along the Philippine Trench.

All these data suggest that tears in subducted lithosphere appear to be the exception rather than the rule, except where tears are necessary, such as where trenches are terminated by transforms, or where there is a reversal in polarity of subduction along an arc. The intense contortion of the Wadati-Benioff zones in regions like northern Tonga (Figure 18) and beneath the Banda Sea (Figure 17) support the contention that subducted slabs deform ductilely. If we are correct in our assertion that ductile deformation is the dominant process controling lateral changes in the structure of subducted lithosphere, it probably controls downdip deformation as well.

What causes segmentation? *Cross and Pilger* [1982] studied the effects of various phenomena on the geometry of subduction. They concluded that the most important factors controlling subduction geometry included convergence rate, absolute motion of the upper plate, subduction of aseismic bathymetric ridges, age of the descending plate, accretion of sediments, and duration of subduction. The only one of these six factors which seems to play a major role in causing and/or controlling lateral segmentation is the subduction of aseismic bathymetric ridges. However, not all PSBs correspond to bathymetric ridges, and they cannot account for all, or even most, segmentation.

For one reason or another, most of *Cross and Pilger*'s [1982] factors are inadequate to explain lateral segmentation at deep or intermediate depths. The accretion and subduction of sediment are clearly important in controlling the shallow structure of subduction in some regions [*Shreve and Cloos*, 1986], but there is no evidence that intermediate or deep segmentation can be correlated with changes in accretion or sedimentation. The age of the descending plate and the duration of subduction are factors that change only slowly along most trenches, and we find no indication that segmentation relates directly to any changes in these factors.

Convergence rate and the absolute motion of the upper plate also change too slowly along most arcs to account for abrupt lateral changes in structure, except where triple junctions occur. Where triple junctions do occur, such as along the Middle America Arc [*Burbach et al.*, 1984] or at the Japan/Izu-Bonin corner, changes in these factors may be very important in controlling segmentation.

There are many bathymetric ridges which are being subducted at various trench systems (Figure 2). These ridges include the following: The Carnegie Ridge, the Nazca Ridge, and the Juan Fernandez Ridge at the South American Trench [*Barazangi and Isacks*, 1976; *Pilger*, 1981; *Pennington*, 1981]; the Cocos and Tehuantapec Ridges and the Orozco Fracture Zone at the Middle America Trench [*Burbach et al.*, 1984; *LeFevre and McNally*, 1985]; the Louisville Ridge at the Tonga-Kermadec Trench [*Billington*, 1980; *Louat and Dupont*, 1982; *Hamburger and Isacks*, 1985]; and the D'Entrecasteaux Fracture zone at the New Hebrides Trench [*Chung and Kanamori*, 1978*a*, *b*], as well as many others. Indeed, about 34% of all PSBs and 5 of the best 12 PSBs show some correlation with bathymetric features impinging on the trench.

This correlation supports the assertion that the subduction of bathymetric features controls the geometry of subduction. However, most PSBs are not located near subducting bathymetric ridges. Furthermore, there are enough bathymetric ridges and enough well constrained PSBs that, in some cases, this correlation may be coincidental. Nevertheless, in many

cases the correlation is very well supported not only by the seismicity data, but by other factors as well [*Kelleher and McCann*, 1976; *Vogt et al.*, 1976; *Cross and Pilger*, 1982].

A seventh factor which can affect subduction geometry is the lateral strain due to the three-dimensional geometric constraints of subduction. Clearly, most subduction zones do not follow the strict rule that the dip equals half the arc radius as proposed by *Frank* [1968], but as we will discuss later, there is actually a fairly broad range of dip angle-arc radius combinations which yield relatively low lateral strain. This fact indicates that, in most regions, lateral strain will not be important in controlling subduction geometry.

However, in regions where there are abrupt changes in trench geometry, the associated large lateral strains can produce major changes in the geometry of the subducted plate. The clearest case occurs at the Hokkaido corner (Figure 14), where a concave-seaward cusp is created by the junction of two convex seaward trenches, the Kurile and Japan trenches. Maintaining a constant dip of 55° across this corner would require about 65-75% lateral shortening. In the observed geometry, the plate appears buckled along an axis roughly parallel to the direction of convergence. The resulting dip at the corner is reduced to about 30°, and the modeled strains are reduced to about 30%. A similar corner with a similar apparent buckling exists at the Japan/Izu-Bonin junction, although this junction is complicated by the presence of a major triple junction. The result is that the dip of the whole Japan segment is much shallower than the average dip for that region, largely due to the geometry of the trench.

Lateral Strain

For idealized trench geometries, there exists a surprisingly broad range of geometries for which the modeled lateral strain is relatively small, even though it is zero only when the arc radius and dip angle satisfy *Frank*'s [1968] argument (Figure 4). For small dip angles (<30°), there is relatively little strain (<10%), no matter what arc radius is involved. Also, for moderate arc curvatures (30° > radius > 60°), the strain is relatively small for any dip angle. There exist only two geometric situations which require very large strains. For small arc radii and steep dips, the models indicate that the subducted plate must undergo considerable lateral extension. For arcs which are concave seaward instead of convex (radius <0.0°) and for steep dips, the plate must accommodate large amounts of lateral shortening. Although Figure 4 represents only the case where the pole is 90° from the trench and subduction is orthogonal, these general results hold for other cases as well.

How much lateral strain do observed subduction geometries require? For observed Wadati-Benioff zone geometries, the modeled lateral strains range from about 50% compression to nearly 100% extension; however, these extremes are misleading. Many of the very large extensions are due to abrupt changes in the dip of the plate. Similarly, abrupt changes in trench geometry, particularly concave seaward bends, cause many of the large compressions. In some cases, large extensions are adjacent to large compressions, which may indicate regions where this simple modeling is inadequate. Even these large strains, however, are not unreasonable when one considers that these strains are accommodated over 10 million years of subduction. A 50% strain over 10 Ma is equivalent to a strain rate of 1.6×10^{-15} per second, which is well within the range of acceptable geologic strain-rates. A 10% strain corresponds to a strain-rate of only 3.2×10^{-16} per second. The total lateral strain predicted for most whole arcs is relatively low, on the order of 10-15% or less, and in several cases is nearly zero.

How does subducted lithosphere accommodate the lateral strains produced by the subduction process? As mentioned previously, where modeling predicts large compressional strain, the plate appears to buckle. Where large extensional strains are predicted, one might expect either ductile stretching of the plate, or tearing. While the available evidence is not conclusive, it seems that ductile deformation is the more likely process.

The CMT focal mechanisms show that downdip stresses generally dominate the lithospheric failure process, especially for deep earthquakes. However, in many cases the lateral strains are observable, and in some cases are even dominant. Comparison of the CMT mechanisms to the lateral strains predicted by the modeling leads to the following generalizations:

1. In regions of low predicted lateral strain, such as South America (Figure 9), there is little or no evidence of lateral strain in the focal mechanisms. *P* and *T* axes are oriented either downdip or normal to the plate (Figure 8*b*).

2. In regions of moderate extensional strain, such as the Kurile-Kamchatka Arc (Figure 14), there is still little effect on the focal mechanisms. Most events still show either downdip or normal *P* and *T* axes (Figure 8*a*).

3. In regions of moderate compressional strain, such as the Sumatra-Java Arc (Figure 17), many focal mechanisms indicate lateral compression in the plate. Downdip stresses no longer clearly dominate the stress regime except for the deepest events (Figure 8*c*).

4. In regions of large extensional strain, such as the Mariana's Arc (Figure 15), most focal mechanisms show lateral tension. Lateral stresses dominate the stress regime, even for deep events (Figure 8*d*).

5. In regions of large compressional strain, such as the Hokkaido corner (Figure 14), the plate tends to accommodate the strain by buckling. Near the buckling axis, bending stresses dominate the focal mechanisms, and most events will indicate lateral tension (Figure 8*e*). Away from the bending axis, downdip stresses dominate, and *P* and *T* axes are either downdip or normal to the plate.

6. In some regions, there is great lateral deformation of subducted plates that does not appear to relate directly to the trench geometry. In northern Tonga (Figure 18), where the deep part of the plate is extremely deformed, the downdip stresses still clearly dominate the focal mechanisms. Although there are also many anomalous events, they show no clear pattern with respect to the strains predicted by the modeling. At the eastern end of the Java subduction zone, beneath the Banda Sea (Figure 17) where the plate is either being deformed or two subducting plates are colliding, the lateral strains dominate the focal mechanisms. Most events show clear lateral compression.

Implications for Driving Mechanisms

What role do subducted plates play in mantle convection and the driving of plate tectonics? Several investigators have shown that "slab pull", the force exerted on plates by the sinking of dense lithosphere at subduction zones, can explain

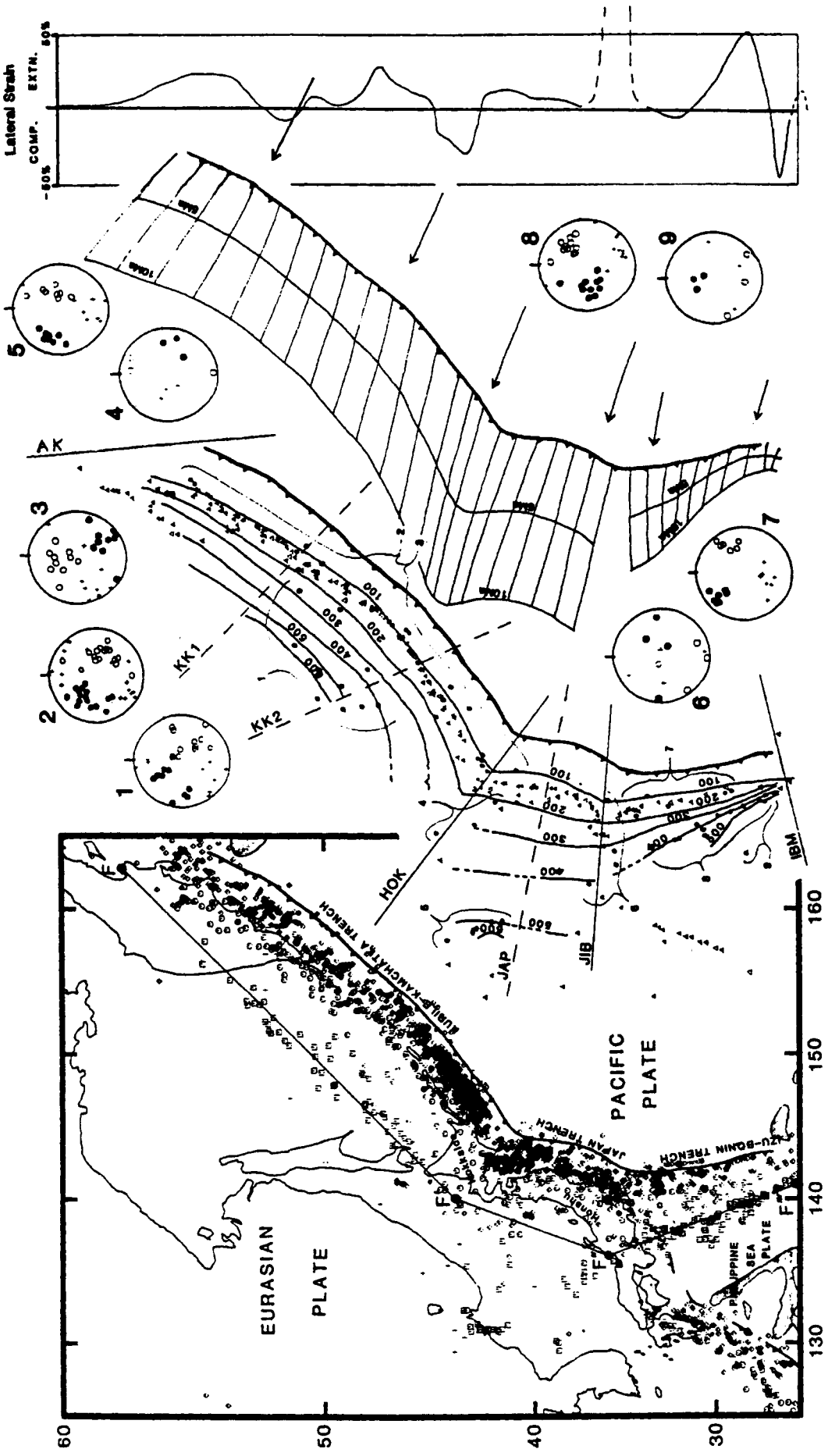

Fig. 14. Results of this study for the northwest Pacific.

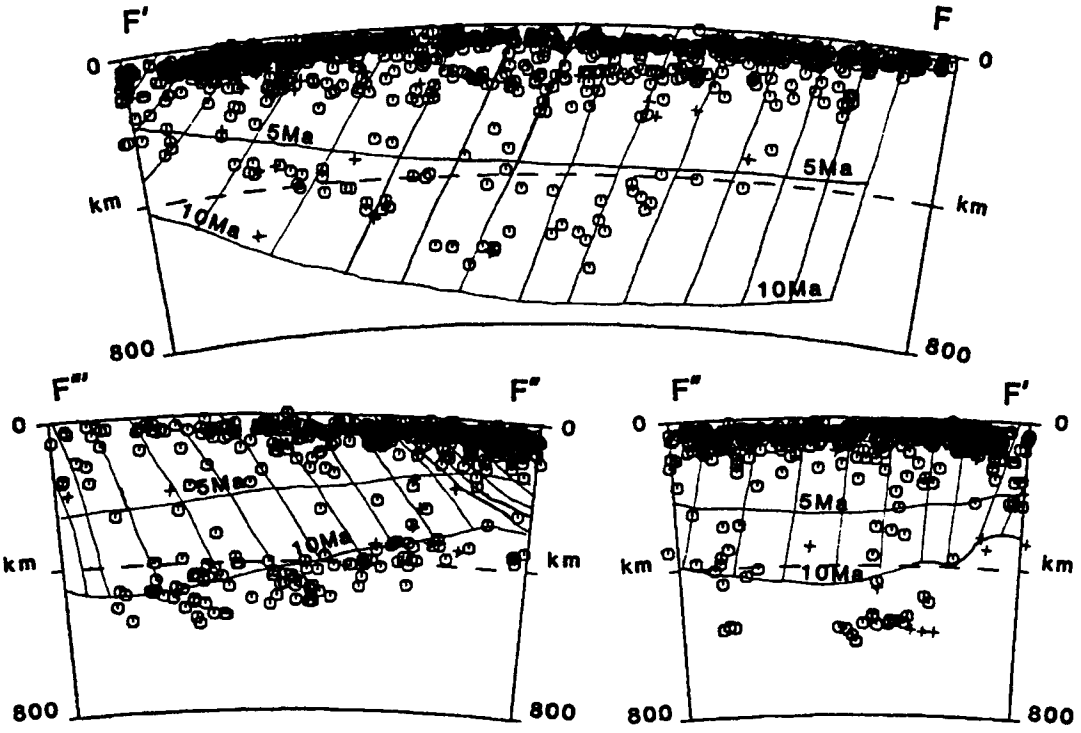

Fig. 14. (continued)

most observed plate motions [*Forsyth and Uyeda*, 1975; *Chapple and Tullis*, 1977; *Carlson*, 1981]. Others have shown that some aspects of subduction geometries can be explained by modeling instantaneous mantle flow [*Hager and O'Connell*, 1979; *Hager et al.*, 1983].

The results of this study support the contention that subducting plates are rigid and remarkably cohesive. Even in cases of large lateral strain, most subducting plates appear to remain continuous and, where possible, deform in ways that conserve the surface area of the plate, for example, by buckling at the Hokkaido corner. This condition is necessary if slab pull acts as the primary driving force, but not if mantle flow acting on the bottoms of the plates is the primary driving force.

Giardini and Woodhouse [1984] have shown that the highly contorted structure beneath northern Tonga can be explained as shear deformation due to flow in the mantle. If this type of deformation were common, it would indicate that subducting lithosphere is not rigid, but very ductile, and it would strongly support mantle flow as the primary driving mechanism. We find no evidence of this type of deformation except beneath Tonga, and possibly beneath the Banda Sea. Interference of mantle flow with subduction may account for some anomalous geometries, such as beneath the Mariana Arc, but most subduction zones have geometries that require little lateral shear.

REGIONAL SUMMARIES OF RESULTS

South America (Figure 9)

The structure delineated by the intermediate-depth seismicity along western South America is highly variable, with dips ranging from about 10° to about 35°. The presence of clusters of events complicates the interpretation of the Wadati-Benioff zone structure in this region. Of the eight PSBs in this region, five (SA1-SA5) were extremely well defined. Our results generally agree with those of *Barazangi and Isacks* [1976, 1979*a*], *Pennington* [1981], and *Swift and Carr* [1974], all of whom separated this region into several segments of varying dip. There are, however, some differences in the number and location of the PSBs delineated in this study and the boundaries proposed by previous investigators (Figure 5).

In the Colombia-Ecuador region this study generally agrees with *Pennington* [1981]. However, this study shows that *Pennington*'s northeast-dipping Ecuador segment (SA1-SA2) is the northern part of a segment whose southern portion dips nearly due east, but which is deformed so that its northern corner dips northeasterly. The northernmost PSB, SA1, coincides with the northern terminus of active volcanism, which continues smoothly across SA2 with a slight bend until it terminates above the deformed corner of the Ecuador segment.

South of Ecuador are three PSBs, SA3, SA4, and SA5, which are well defined. SA3 looks more like a sharp contortion of the plate than a tear, but clear resolution of this structure is impossible using only teleseismic data. *Warsi et al.* [1983] and *Hilde and Warsi* [1982] noted extensional structures across the Mendana Fracture Zone just offshore of SA3. They suggested that the lateral stresses caused by subduction and segmentation of the Nazca Plate induced rifting along this fracture zone. This implies that SA3 is a tear.

Barazangi and Isacks [1976, 1979*a*] proposed a single major segment boundary at the northern terminus of the Chilean volcanic line, which is between SA4 and SA5. SA5 corresponds to the major concave seaward bend in the trench axis. *Hasegawa and Sacks* [1981] concluded from the local network data that there was no tear in the plate, but that the plate was smoothly contorted across this region, a conclusion confirmed independently by *Grange et al.* [1984*a*, *b*]. Focal mechanisms determined from local network data in this region

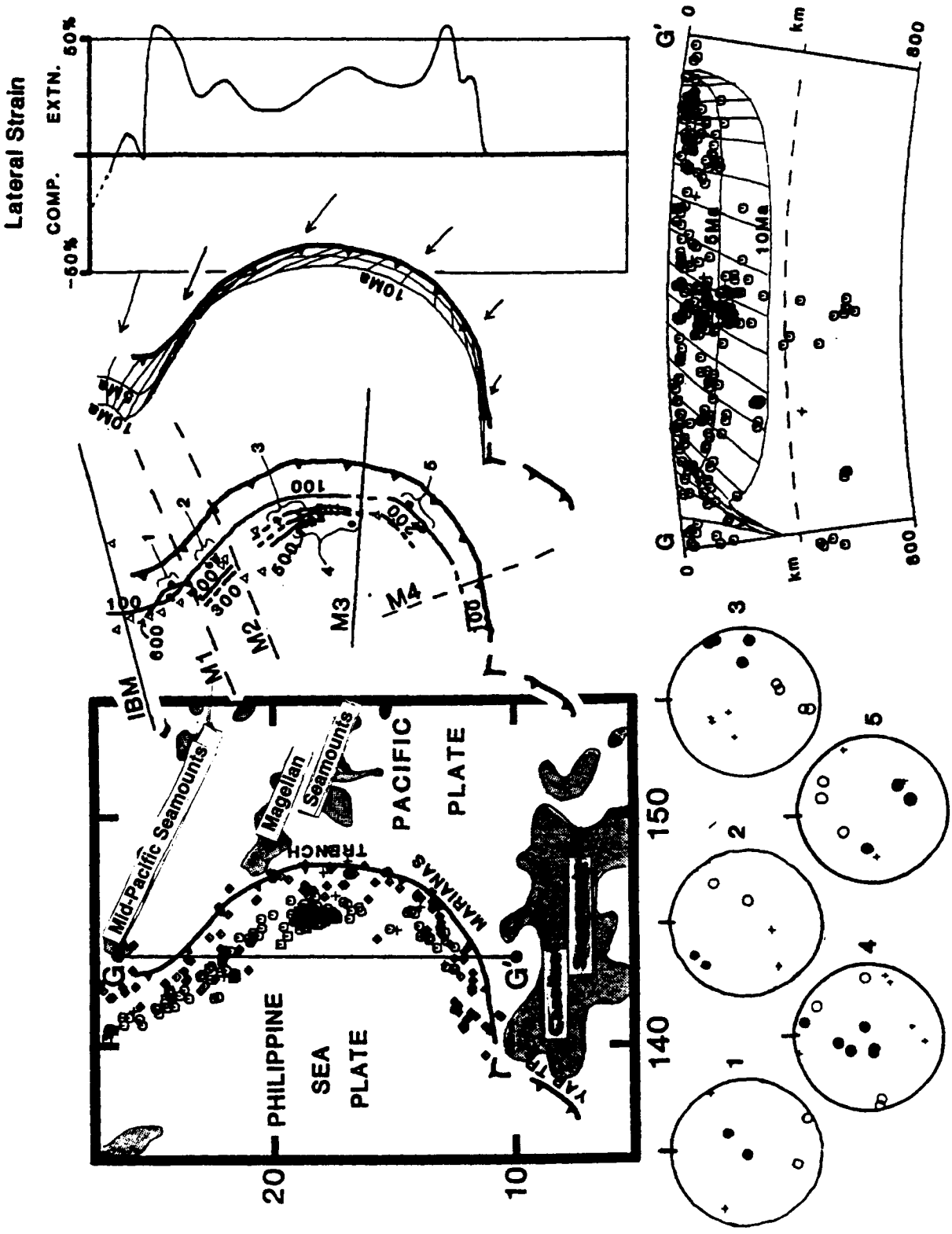

Fig. 15. Results of this study for the Mariana Arc.

[*Schneider*, 1984] are also consistent with a contorted structure, rather than a tear. *Yamaoka et al.* [1986], however, found it difficult to fit this structure with an inextensible vinyl shell without a tear.

The three other poorly defined PSBs, SA6, SA7, and SA8, coincide loosely with the tears proposed by *Swift and Carr* [1974]. SA6 is just north of the boundary proposed by *Barazangi and Isacks* [1976; 1979*a*], near the southern terminus of the Chilean volcanic line. SA7 corresponds to the northern end of active volcanism in southern Chile. SA8 occurs in a region where the intermediate-depth activity disappears gradually.

An interesting feature of the seismicity along western South America is the pattern of deep (>600 km) activity. There are two very active regions of deep seismicity beneath South America, one approximately parallel to and east of the subduction in Peru, and the other east of and parallel to the "normal" subduction beneath northern Chile. The ISC-*pP* data include one exceptionally large (m_B = 7.5) isolated deep earthquake which occurred beneath Colombia on July 31, 1970 [*Furumoto*, 1977]. Although the ISC reports no events occurring within several hundred kilometers of this event since 1964, the historical data include two other deep events in this region. These events do not correspond to an extension of the intermediate-depth structure in any obvious way.

In all three regions of deep seismicity, there is virtually no activity between about 300 and 600 km. This gap is characteristic of many Wadati-Benioff zones, but nowhere is it more prominent than in South America. The deep earthquakes (>300 km) do not lie on the direct extension of the Wadati-Benioff zone as defined by the intermediate-depth activity above them. Rather, to fit the deep events into a continuous structure there must be a major downward bend of the subducted plate just below the end of the intermediate-depth activity. Although this bend may be barely visible in the local network locations of *Hasegawa and Sacks* [1981], it is not visible in the teleseismic data.

Generally the modeling finds lateral strains that are 5% or less for the South American subduction zone, except in a few places where larger extensions occur because of abrupt changes in dip. The generally small lateral strains occur because of the shallow dip of the descending plate (for example, Figure 4). North of central Peru the plate is in a state of slight extension, but from central Peru south the subducted slab is in weak compression. Near southern Peru there is a major concave-seaward bend in the trench where the modeling predicts compressive strain of roughly 20%. This amount of shortening is smaller than one might expect for such a major bend in the trench, because of the shallow dip.

CMT focal mechanisms for this region are consistent with the modeling, showing no evidence of significant lateral stresses. The deep events (groups 6 and 11) have compression axes which are downdip to, and tension axes which are normal to, the Wadati-Benioff zone. The intermediate-depth events south of the major bend in the trench (groups 7, 8, and 9) almost all have downdip tension axes and normal compression axes. North of the bend the intermediate-depth events (groups 1-5) have a mixture of downdip compression and downdip tension axes with opposite axes oriented normal to the plate.

Middle America (Figure 10)

There are three PSBs along the Middle America Arc. MA1 is extremely well defined and clearly separates the Wadati-Benioff zone into two major segments. This structure is consistent with that proposed by *Molnar and Sykes* [1969], and by *Burbach et al.* [1984]. Other investigators [*Stoiber and Carr*, 1973; *Dean and Drake*, 1978; and *Carr et al.*, 1979] have proposed a more extensively segmented model (Figure 5), but extensive segmentation is not evident within the resolution of the teleseismic data.

North of MA1, the seismicity extends to a depth slightly greater than 100 km with a very shallow dip (20°-30°). The active volcanoes are inland from the deepest extent of the Wadati-Benioff zone, forming a broad and discontinuous band of volcanism. South of MA1, the Wadati-Benioff zone is more clearly defined and extends to well over 200 km depth. The dip along this segment varies from about 60° in the south to about 45° in the north.

Beneath Guatemala there is a very poorly defined PSB, MA2. The volcanic chain is continuous across MA2, but there is a cluster of volcanoes above MA2 which appear to be aligned with it. The volcanic chain ends abruptly between MA1 and MA2, near the boundary between the North American and Caribbean plates. This cessation of volcanism may be related to the change in overriding plates, rather than a change in the structure of the subducting plate [*Burbach et al.*, 1984].

Another poorly defined PSB, MA3, occurs at the southern end of the Middle America Trench. This PSB is the southeastern limit of the Wadati-Benioff zone observed in the teleseismic data. MA3 roughly corresponds to a segment boundary proposed by *Matumoto et al.* [1976], *Liaw* [1982], and *Burbach et al.* [1984]. Although there is evidence of subduction beneath Panama [*Adamek and Pennington*, 1984], it is not visible in the ISC-*pP* data.

Modeling of Middle American subduction was complicated by the fact that there are two overriding plates, requiring different poles of rotation for the southern and northern parts of the subduction zone. Although the triple junction is not well defined, we place it at the bend in the trench near the Gulf of Tehuantepec. This bend forms a small concave-seaward cusp in the trench, which produces a strong compressional strain. In this case the difference in rotation poles increases the predicted strain to well over 50% compression. However, since this triple junction is unstable, the changing trench geometry may accommodate some of this strain.

Because of the shallow dip of the slab to the north of MA1, the modeling predicts small extensional strains. The CMT mechanisms are inconsistent, with two events having nearly vertical compression and normal tension axes, one event having downdip compression and lateral tension axes, and one event having lateral compression and normal tension axes (groups 1 and 2).

South of MA1, the geometry of the Wadati-Benioff zone is better defined and has a steeper dip. Here the modeling predicts strains ranging from about 30% extension to about 40% compression. These large strains are caused by the steep dip and the changes from convex-seaward to concave-seaward to convex-seaward curvature, and may be an artifact of the modeling procedure. The CMT mechanisms show fairly consistent downdip tension and normal compression for this entire part of the arc (group 3).

Eastern Caribbean (Figure 11)

The North American Plate is subducting beneath the Caribbean Plate along the Lesser Antilles Arc. The Wadati-

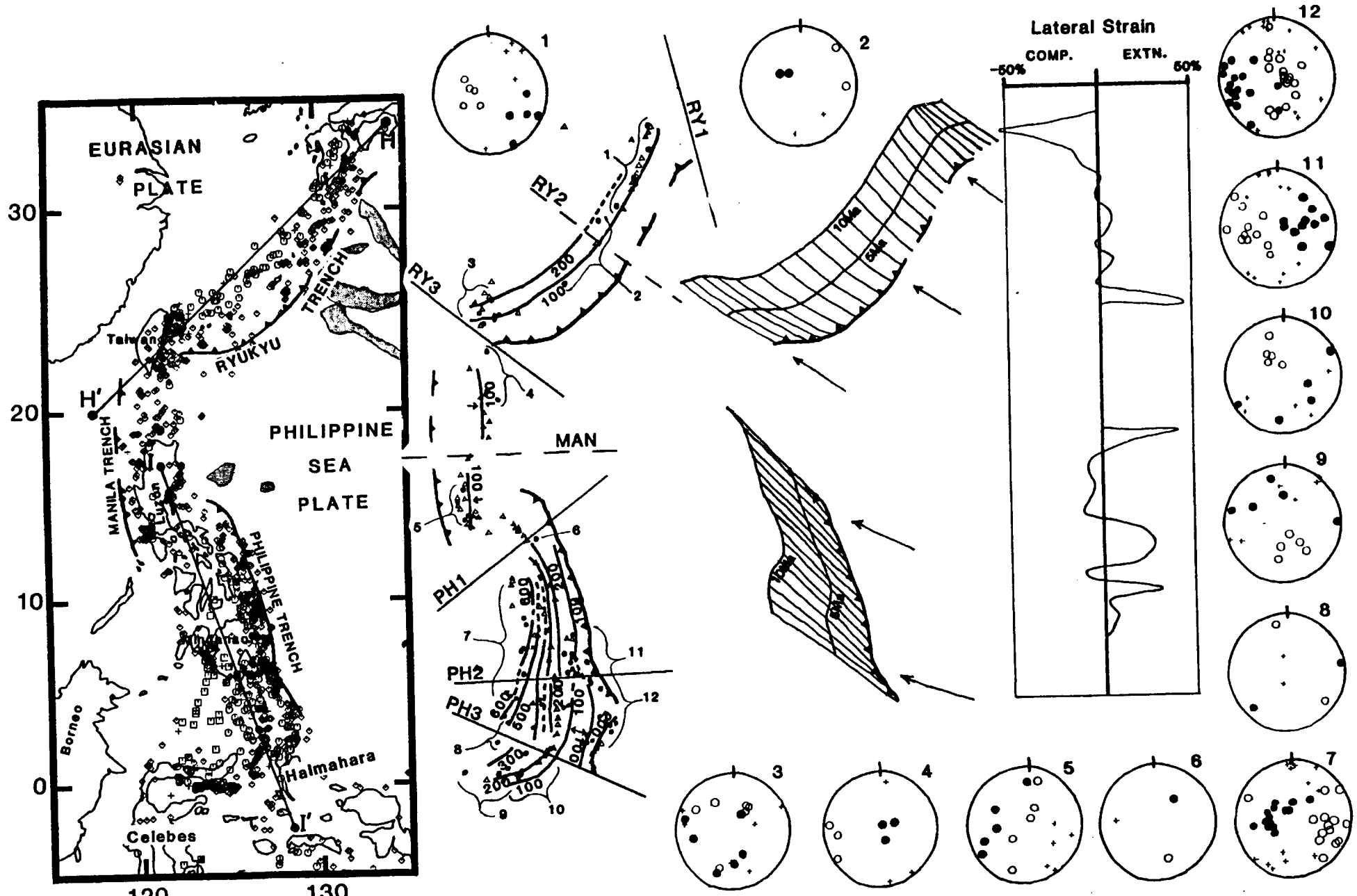

Fig. 16. Results of this study for the western Philippine Sea.

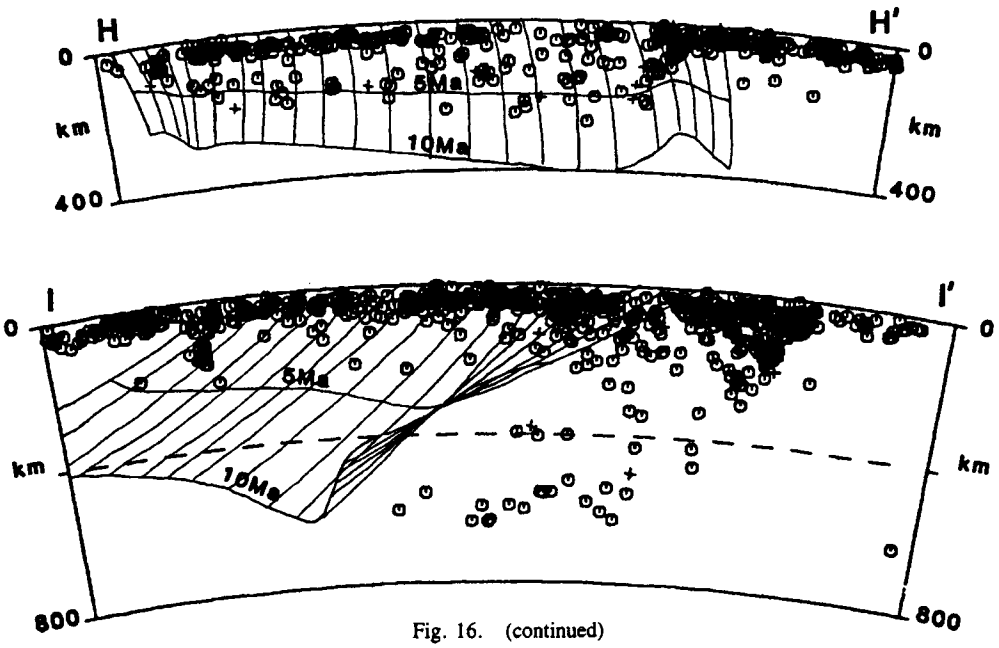

Fig. 16. (continued)

Benioff zone extends to a depth of only a little over 100 km, with a dip of about 25°-30° beneath the central part of the arc. This study generally agrees with *Dorel* [1981] and *Stein et al.* [1982] who interpreted the structure in this region to be continuous.

Along the Puerto Rico Trench the relative motion between the plates is nearly parallel to the trench [*Minster and Jordan*, 1978], but the intermediate-depth seismicity clearly indicates a southward dipping Benioff zone. This structure is consistent with the results of *Murphy and McCann* [1979], *Frankel et al.* [1980], and *McCann and Sykes* [1984]. The modeling of this region predicts very small strains (less than 5%) because of the shallow dip.

In the eastern Caribbean the ISC-*pP* data allow us to delineate three PSBs. The southernmost, EC3, is the best defined, although the structure to the south of it is not clear. EC3 also corresponds to the southern end of the active volcanism along the Lesser Antilles. EC2, the PSB east of Puerto Rico, is poorly defined. Local network data in this region [*McCann and Sykes*, 1984] show no sign of a boundary, although EC2 is near the northern terminus of active volcanism along this arc. The PSB in the Mona Passage region, EC1, is not well defined because the geometry of the segment to the west is not clear. This PSB corresponds to a tear postulated by *McCann and Sykes* [1984] separating continuous subducted lithosphere beneath Puerto Rico from a possible block of detached lithosphere to the west.

South Sandwich Arc (Figure 12)

The subduction of the South American Plate beneath the South Sandwich Arc is poorly defined, because the South Sandwich arc is so distant from most seismic stations. However, the Wadati-Benioff zone extends to a depth of slightly over 200 km and has a dip of 25°-35°. The present study finds two PSBs, SS1 and SS2, separating the Sandwich Arc into three segments. These segments may correspond to the three regions described by *Frankel and McCann* [1979] on the basis of aftershock zones. Both PSBs coincide with significant changes in the volcanic line. SS1 also corresponds to a tear proposed by *Yamaoka et al.* [1986].

The northernmost segment is the most seismically active, and has an unusual geometry. Its strike is nearly perpendicular to the portion of the trench lying just to the east. It dips toward the southeast, indicating that it is attached to the surface plate along the nearly east-west portion of the trench lying to the north. This segment might represent the slightly subducted edge of the nonsubducting block, and SS1 would then be the hinge fault postulated by *Forsyth* [1975]. Several of the CMT mechanisms near SS1 could be interpreted as hinge-faulting.

SS2 is less well constrained than SS1 because of the low seismicity rate. Here the change in strike of the subducted slab corresponds to the change in strike of the trench, although it appears to be more abrupt. SS2 occurs near the change in focal mechanisms noted by *Forsyth* [1975], which is also visible in the CMT mechanisms. The modeling for this arc predicts small strains, which reach a maximum of about 15% near the southern end of the arc.

Alaska-Aleutian Arc (Figure 13)

The Alaska-Aleutian Arc has a well defined Wadati-Benioff zone that extends to depths of about 250 km. Beneath the central Aleutians, the subducted plate has a fairly simple structure, with a dip of about 60-65°. The dip shallows eastward along the arc to about 45° beneath the Alaska Peninsula, and finally to about 25° north of Cook Inlet. This structure is consistent with that delineated by other investigators [*Jacob et al.*, 1977; *Engdahl*, 1977; *Reyners and Coles*, 1982].

Several investigators have proposed segmentation of the Alaska-Aleutian Arc. *Abe* [1972] proposed tears below Amchitka Pass and Amkta Pass, and *Stauder* [1972] used focal mechanisms near Amchitka Pass to conclude that there was a tear. *Spence* [1977] divided the Aleutian Arc into about six blocks, mainly on the basis of bathymetry.

This study finds five PSBs, of which only two are well defined. The best of these, AA5, coincides with the proposed tear at Amchitka Pass [*Abe*, 1972; *Stauder*, 1972; *Spence*,

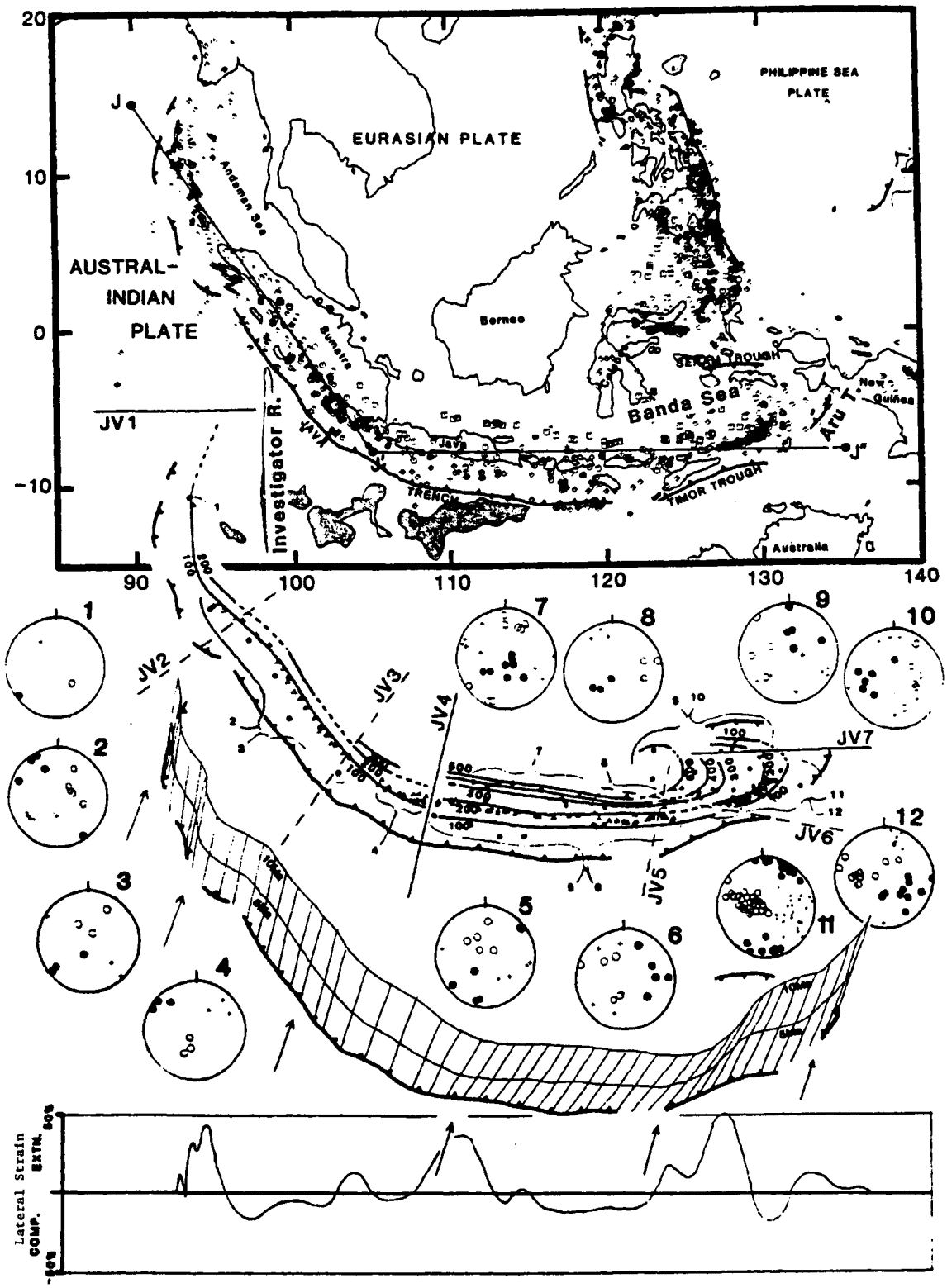

Fig. 17. Results of this study for the Java Arc.

1977]. This PSB is near the western end of the active volcanism along the Aleutian Arc and corresponds to a small but significant bend in the trench axis. West of this PSB, the trench axis is almost parallel to the direction of relative plate motion, making it primarily a transform boundary. The other well defined PSB, AA1, is at the northern end of Cook Inlet. This PSB may correspond to the possible tear suggested by *Pulpan and Frohlich* [1985] on the basis of geometric arguments. *Pulpan and Frohlich* [1985] used local network locations to propose a tear that corresponds to the poorly defined PSB at the southern end of Cook Inlet, AA2. Here a change in strike of the Wadati-Benioff zone occurs along with a change in strike in the volcanic line.

For the Alaska-Aleutian Arc, the strain predicted for 10 Ma of subduction averages to about 10% extension for the whole arc. However, the seismically active slab only extends to a

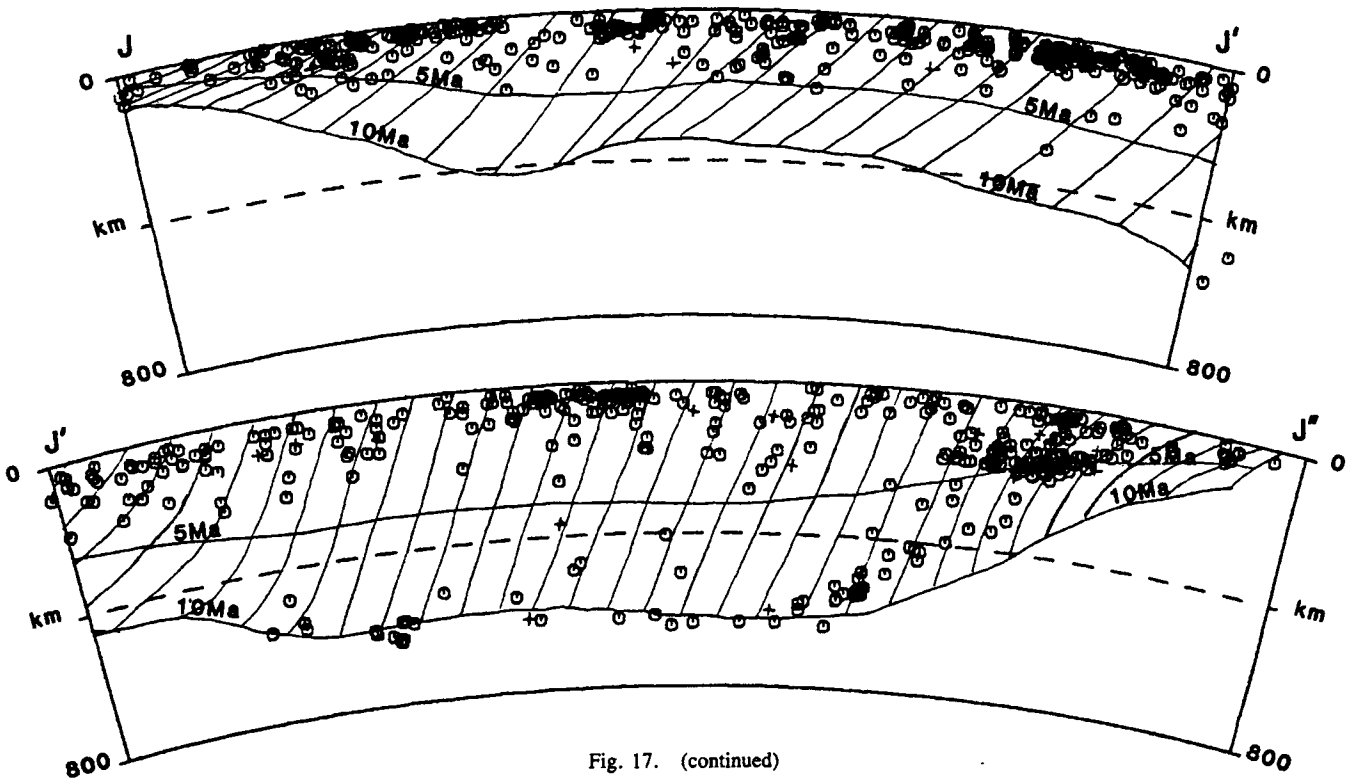

Fig. 17. (continued)

depth of slightly over 200 km, so the actual strain is probably much less. The nine CMT mechanisms for events in this region show no clear pattern.

Kurile-Kamchatka Arc (Figure 14)

Along the Kurile-Kamchatka Arc the structure is very simple, with the dip fairly constant at about 65°. There are only two PSBs along this arc, KK1 and KK2. These PSBs separate the central region, where activity extends to over 600 km, from the regions on either side, where the deepest activity is only about 350 km. Above 350 km the plate appears to be continuous. This interpretation disagrees with that of *Veith* [1974], who delineated numerous tears along the Kurile Arc (Figure 6), but agrees with those of most other investigators [*Isacks and Barazangi*, 1977; *Stauder and Mualchin*, 1976]. In the general vicinity of KK2, *Isacks and Barazangi* [1977] noted a change in geometry, and *Stauder and Mualchin* [1976] noted a change in intermediate-depth focal mechanisms.

The modeling finds lateral strains of between 5 and 25%, averaging about 10% extension for the whole arc. The CMT focal mechanisms have downdip compression and normal tension axes for deep events along the Kurile Arc (group 1), and intermediate-depth events have a mixture of downdip tension and compression axes, with the opposite stress axes oriented normal to the slab (groups 2 and 3). There are only a few events along this arc which have stress axes oriented laterally. There is no clear evidence that events with downdip tension occur only in the north, and that events with downdip compression occur only in the south, as suggested by *Stauder and Mualchin* [1976].

Hokkaido Corner (Figure 14)

The junction between the Kurile and Japan Trenches is the Hokkaido corner, and corresponds to a very well defined PSB, HOK. Across this PSB the subducted slab remains continuous, at least to depths of 300-350 km, but below this depth there is a notable absence of seismic activity. The concave-seaward geometry of this corner requires very large compressional strains. Indeed, if there is a tear or hinge fault associated with this PSB, as proposed by some investigators [*Isacks and Barazangi*, 1977; *Stauder and Mualchin*, 1976], the geometry of this corner requires that the two segments overlap [*Isacks and Molnar*, 1971; *Minamino and Fujii*, 1981]. There is no evidence of any overlap in the teleseismic data, which indicate that the plate is buckled along an axis coincident with HOK, lying roughly parallel to the direction of convergence. *Kanamori* [1971] suggested that there might be a tear, but that the lateral compression across the corner keeps the edges of the two segments together, resulting in the buckling. However, the seismicity data cannot distinguish between this model and a model with no tear at all.

Modeling of the observed geometry predicts shortening in excess of 30% for this corner, which is much less than would be expected if the dip remained constant across the corner. A constant dip of 55° across this corner would require a shortening of about 70%. This smaller modeled strain indicates that the buckling, which produces a shallow dip at the corner and below the Japan Sea, is accommodating a large amount of the lateral shortening. Thus, the trench geometry seems to control the geometry of the subducted plate.

Three CMT mechanisms near HOK and the axis of buckling show lateral tension, i.e., tension axes perpendicular to the buckling axis and compression axes normal to the subducting plate (group 4). These focal mechanisms are consistent with the results of *Sasatani* [1976], who showed that focal mechanisms from this region were consistent with bending stresses in a buckling plate. The absence of events having lateral compression supports the hypothesis that buckling takes up most of the compressional strain.

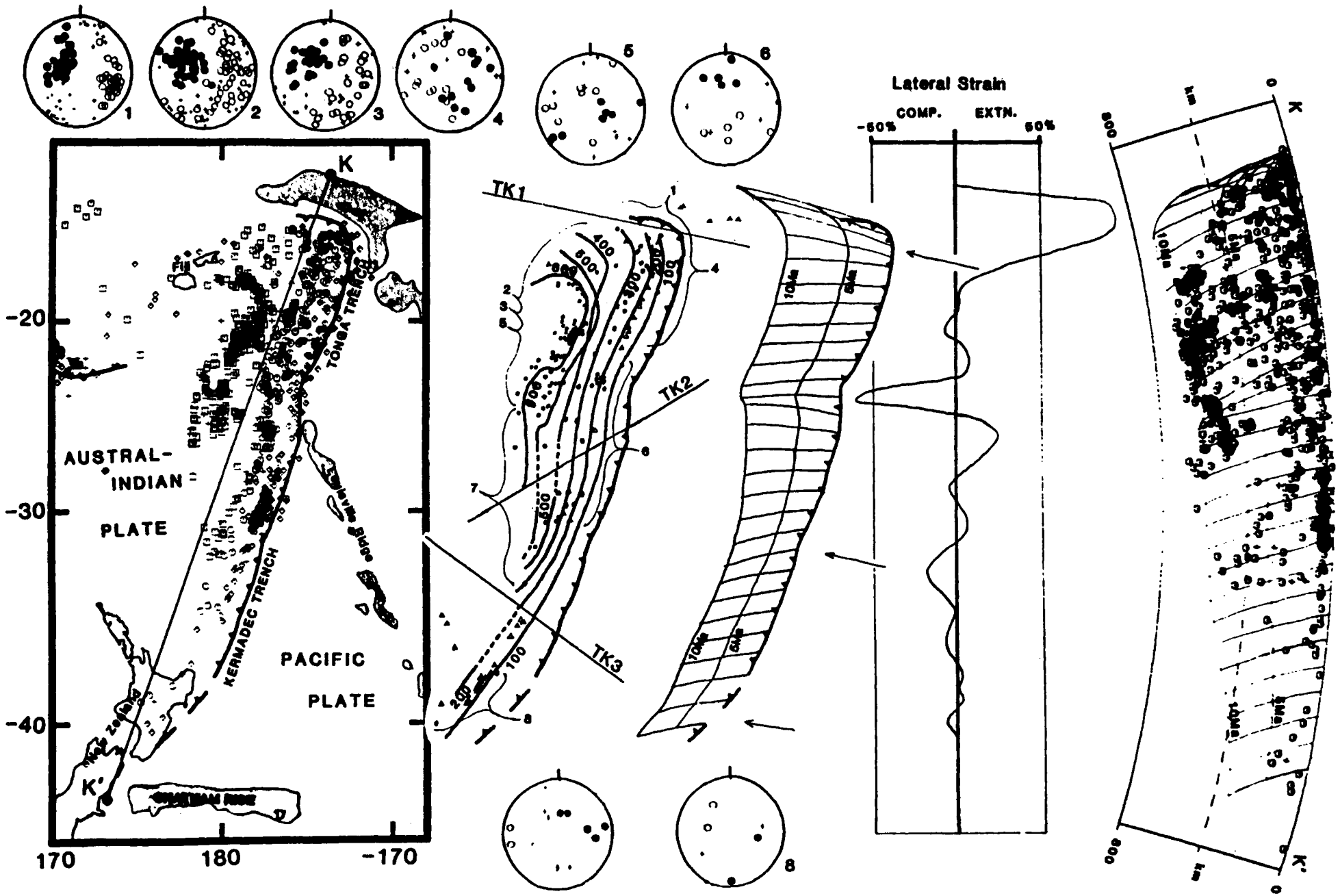

Fig. 18. Results of this study for the Tonga-Kermadec Arc.

Honshu Arc (Figure 14)

The Wadati-Benioff zone beneath Central Honshu and the Sea of Japan extends to a depth of over 600 km and has an average dip of about 35°, except for the deepest part of the northern edge of the segment, which has a steeper dip. The deep seismicity is concentrated along two zones near the edges of this segment, with little activity in between. JAP, which separates these two zones, is a very uncertain PSB because of the remarkably planar geometry exhibited by the two regions together. Most investigators interpret this region as a single continuous segment [*Katsumata*, 1966; *Utsu*, 1971, 1974; *Umino and Hasegawa*, 1982]. However, *Carr et al.* [1973] postulated that tears separated this region into at least four segments (Figure 6). *Kawakatsu and Seno* [1983] also divided this region into four parts on the basis of characteristic seismicity patterns, but they did not postulate any tears separating the parts.

The modeling predicts lateral extension of 5-15% along this arc. All the CMT focal mechanisms for this region are for deep events and have downdip compression axes (group 5). Most of these events have normal tension axes, but a few have nearly lateral tension axes.

Japan/Izu-Bonin Corner (Figure 14)

The junction of the Japan Trench and the Izu-Bonin Trench, JIB, is geometrically and structurally similar to the Hokkaido corner. There is even a similar gap in seismicity below about 300-350 km. A difference is that this corner involves two different overriding plates. There is no evidence of overlap of the segments in the seismicity data; however, between about 200 and 300 km a slight but abrupt change in both the strike and the dip of the seismic zone may indicate that there is a tear. Above 200 km depth, the plate appears to be continuous across this PSB. These results agree with those of Aoki (1974), who found that the plate was continuous to about 150-200 km, but was torn below that depth. *Utsu* [1974] and *Hirahara* [1981], however, concluded from seismicity data that the plate was continuous across this corner to at least 300 km depth.

Even though this junction is concave seaward, the difference in rotation parameters between the two overriding plates produces a large apparent extension in the modeling. Since this triple junction is unstable, the trench geometry must change with time, which may accommodate much of the apparent extension.

Although there is much scatter, the CMT mechanisms nearest this junction have mostly lateral tension axes and mostly normal compression axes (group 6). This is consistent either with lateral extension or, as with the Hokkaido corner, with buckling. One or two of these mechanisms could be interpreted as hinge-faulting.

Izu-Bonin Arc (Figure 14)

The deep seismicity increases again just south of JIB. The maximum depth of seismicity increases southward from about 400 km to about 600 km, and the dip increases smoothly from about 40° to about 80°.

Most of the CMT mechanisms for intermediate and deep events along the Izu-Bonin Arc have downdip compression axes and nearly lateral to lateral tension axes. A slight shift in the orientation of stress axes occurs between the intermediate and deep events, consistent with the change in dip of the plate from north to south.

Izu-Bonin/Mariana Corner (Figures 14 and 15)

The PSB IBM occurs near the intersection of the Izu-Bonin and Mariana Arcs. Here there is a kink in the Wadati-Benioff zone as it becomes vertical and even appears to curl under slightly beneath the northern Marianas. *Isacks and Molnar* [1971] and *Katsumata and Sykes* [1969] noted gaps in the intermediate and deep seismicity in this region, but found no direct evidence for a tear. The modeling finds that large compressive strains occur because of the concave bend of the trench and the steep dip. However, the northernmost part of the Mariana Arc is nearly parallel to the direction of convergence, indicating that this junction may be an arc-transform-arc junction rather than a true arc-arc junction. Although there are no events with CMT mechanisms within 100 km of IBM, the nearest events on either side all show nearly vertical compression and lateral tension axes (group 9, Figure 14; group 1, Figure 15).

Mariana Arc (Figure 15)

Beneath most of the Mariana Arc the structure of the Wadati-Benioff zone is poorly defined. The deep seismicity extends to a depth of over 600 km and occurs in several clusters that are not easy to connect with a smooth continuous structure. Two poorly constrained PSBs, M1 and M2, are defined primarily by the gaps in deep seismicity between these clusters. Just south of IBM, the dip is nearly vertical and the plate even appears to curl under, but the dip decreases to about 60° beneath the central Marianas. These results are consistent with the observations of *Katsumata and Sykes* [1969]. *Horiuchi* [1977] noted that the deepest part of the seismic zone flattens beneath the central Marianas.

A well defined PSB, M3, separates the Wadati-Benioff zone beneath the central Marianas from the poorly defined zone to the south between M3 and the Yap Trench. The ISC-*pP* data do not indicate any seismicity beneath the Yap Trench, although there are two strike-slip focal mechanisms in this region which suggest tearing may occur near the Mariana-Yap junction. M3 corresponds roughly with a tear proposed by *Yamaoka et al.* [1986].

The modeling predicts extensional strains of 25-55%, caused by the small curvature of the Mariana Arc and the extraodinarily steep dip, (for example, Figure 4). The CMT focal mechanisms have mostly lateral tension and normal compression axes for intermediate-depth events beneath the central Marianas (group 3), and primarily lateral tension and either downdip or normal compression axes for intermediate-depth events beneath the southern Marianas (group 5). One deep event near M3 has downdip tension and lateral compression axes, but most of the deep events have vertical compression and lateral or normal tension axes (group 4). The predominance of lateral tension in the focal mechanisms is consistent with the large tensional strains predicted by the modeling.

Ryukyu Arc (Figure 16)

Along the Ryukyu Trench, the Philippine Sea Plate is subducting beneath the Eurasian Plate. The Wadati-Benioff zone extends to only 150-250 km with a dip of 45°-55°. The

teleseismic data do not delineate the subduction zone along the Nankai Trough or indicate how it connects to the subduction zone along the Ryukyu Trench.

There are three PSBs along this arc. RY1 represents the northern end of the Wadati-Benioff zone as well as the northern end of active volcanism. RY2 is poorly defined in the teleseismic data, but it coincides with a break in the trench, and with the southern end of active volcanism. *Shiono et al.* [1980] noted a change in Wadati-Benioff zone structure and in focal mechanisms across the Tokara Channel which may correspond to RY2.

The Ryukyu Trench and the Wadati-Benioff zone terminate very abruptly at the northern end of Taiwan with a very well defined PSB, RY3. There is a broad region of active volcanism just north of this PSB and above a region of high seismic activity. This PSB corresponds to a tear proposed by *Yamaoka et al.* [1986].

The modeling predicts lateral strain for the Ryukyu Trench that is generally less than 10%. There is a region of large compressional strain where the Ryukyu Trench intersects the Nankai Trough. However, the trench geometry and the nature of this junction are not well defined, and the seismicity in this region does not extend much below about 100 km depth. Just north of Taiwan the modeling finds extensional strains of as much as 50% caused by a westward bend in the trench. This value is probably too high, since the seismically active slab only extends to slightly over 200 km depth, and since the slab may have a free edge just to the south.

CMT mechanisms for most events along the northern Ryukyu Arc have downdip tension and normal compression axes (group 1), and two events near the central Ryukyu Arc have downdip compression and nearly lateral to lateral tension axes (group 2). CMT mechanisms for events near Taiwan show no systematic orientation of stress axes, but a few of these events may indicate hinge faulting (group 3).

Manila Trench-Luzon (Figure 16)

South of Taiwan, the shallow activity trends nearly north-south, and the few intermediate-depth earthquakes there delineate a shallow, eastward dipping Wadati-Benioff zone. This Wadati-Benioff zone probably represents subduction of the South China Sea beneath the Manila Trench. CMT mechanisms for events in this region have compression axes dipping steeply to the east and tension axes dipping shallowly to the west.

At the northern end of Luzon is a poorly defined PSB, MAN. South of this PSB the intermediate-depth activity is sparse, but it appears to delineate a shallow, westward dipping Wadati-Benioff zone. There is a clear offset in the volcanic line across this PSB, and the Manila trench becomes better defined to the south. CMT mechanisms from this region have compression axes oriented mostly toward the west or southwest, and tension axes either nearly vertical or north-south (group 5).

Philippines (Figure 16)

The Philippines are one of the most complicated subduction zones. The structure delineated in this study is similar to that found by *Cardwell et al.* [1980]. There are three well defined PSBs. PH1 defines the northern end of the Philippine Wadati-Benioff zone. The CMT mechanism for the event closest to PH1 may indicate hinge faulting (group 6). To the south of PH1 the maximum depth of seismicity increases quickly to about 550 km, with a prominent gap between about 350 and 500 km in the northern part of this region. Modeling of the northern Philippine Trench finds strains ranging from about 10% shortening to about 30% extension.

The structure becomes more complicated to the south. PH2, near the southern end of the Philippine Trench, marks the northern boundary of a second shallow-dipping Wadati-Benioff zone which dips to the east beneath Halmahera to a depth of just over 200 km. South of PH2 the active volcanism forms two clear volcanic lines, one over the westward dipping seismic zone and the other over the eastward dipping zone. Most of the CMT mechanisms for events associated with the eastward dipping zone have tension axes dipping steeply to the east or south and compression axes dipping shallowly to the west (group 12).

PH3 marks the southern end of the eastward dipping seismic zone coinciding with a significant offset and change in structure of the westward dipping zone. At least one of the two CMT mechanisms near this PSB may indicate hinge faulting (group 8). CMT mechanisms for events south of PH3 have either downdip tension or normal tension axes with scattered compression axes (groups 9 and10).

Sunda Arc (Andaman-Java-Banda Sea) (Figure 17)

The Indo-Australian Plate subducts northward along the Java Trench from the Andaman Sea to the Banda Sea. Beneath the Andaman Sea, subduction is highly oblique, producing complicated back-arc tectonics [*Eguchi et al.*, 1979]. Here the Wadati-Benioff zone extends to slightly over 100 km depth. Beneath Sumatra the Wadati-Benioff zone extends to about 200 km depth with a dip of about 45°, and beneath Java it extends to about 600 km depth with a dip of about 60°. Beneath the Banda Sea the structure is much more complicated.

This study delineates several PSBs along this arc. JV1 is the northern end of the Wadati-Benioff zone. JV2 and JV3 are poorly defined, although major changes in trench geometry and volcanism occur near JV2. JV4 is very well defined, although it is associated with less significant changes in volcanism and trench geometry.

JV5 is poorly defined, however; it coincides with the break between the Java Trench and the Timor Trough, and with a major change in the volcanic line. JV6 is a slightly better defined PSB at the other end of the Timor Trough, which is nearly perpendicular to JV5. JV6 corresponds to a tear proposed by *Yamaoka et al.* [1986]. These two PSBs separate events in the northward dipping slab from events within part of a westward dipping slab subducting along the Aru Trough. This westward dipping slab extends to over 600 km depth with a dip of about 35°-40°.

The transition between the northward and westward dipping slabs occurs between JV5 and JV6 along the Timor Trough, but the nature of this transition is unclear. The shallow and intermediate-depth activity in the westward dipping slab possess a slight curvature toward the other slab, suggesting that they may be continuous. However, an apparent gap in the volcanic line, and between the two groups of events, suggests that they are not continuous. Most investigators [*Hamilton*, 1979; *Cardwell and Isacks*, 1978; and *Papp*, 1980] interpret the subducted plate between the Java and Aru segments to be continuous.

On the north side of the Banda Sea, there are a few shallow

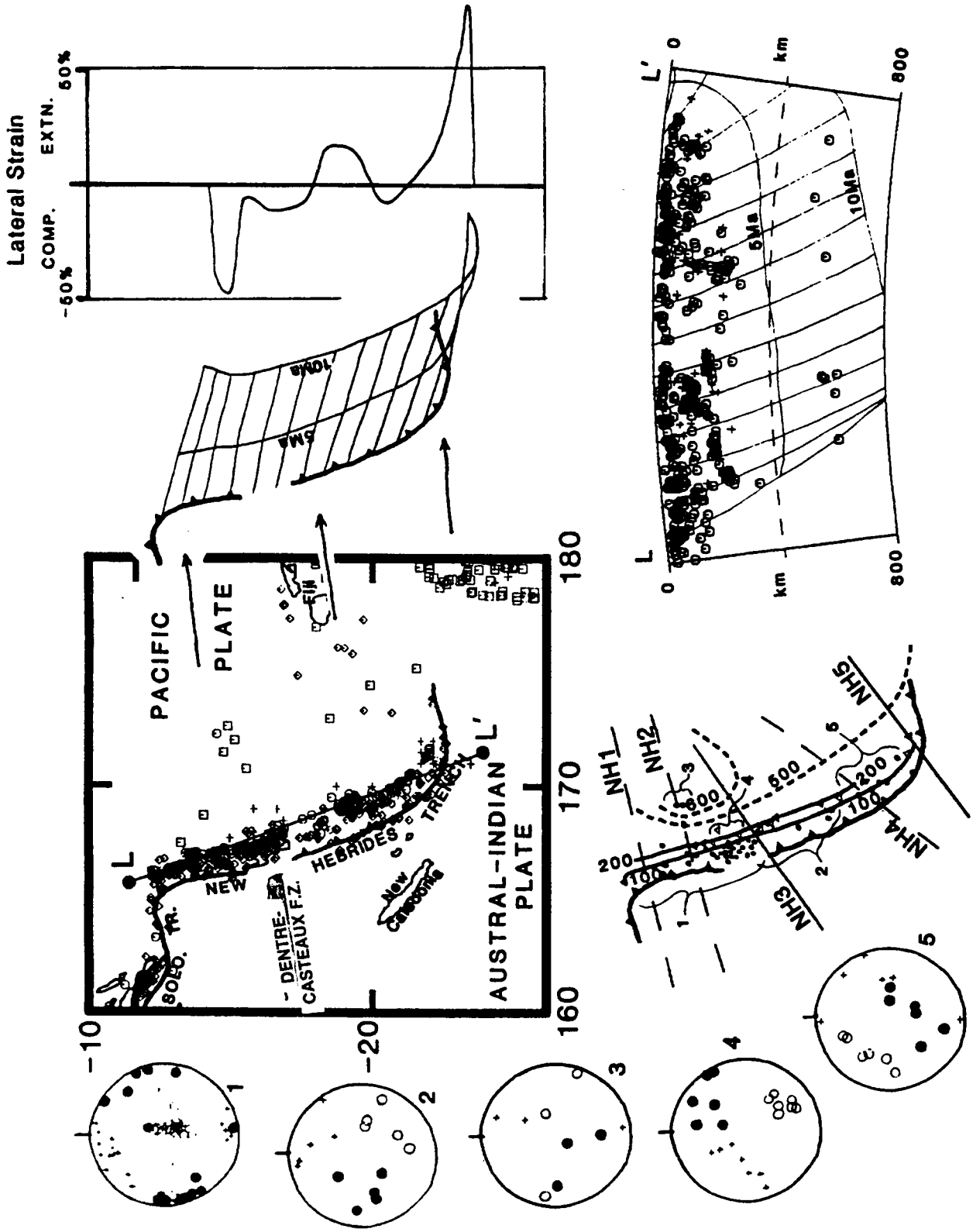

Fig. 19. Results of this study for the New Hebrides Arc.

and intermediate-depth events which suggest that there is subduction to the south along the Seram Trough, at least to depths of about 300 km. There are also a few deep (>600 km) events lying too far north and too far west to fit easily into any of the other structures. *Hamilton* [1979] and *Papp* [1980] interpret these events as a continuation of a single contorted slab subducting beneath the Java-Timor-Aru-Seram Trench, producing a spoon-shaped subducted plate. However, *Cardwell and Isacks* [1978] argue that this arrangement is geometrically impossible. They interpreted the intermediate seismicity beneath the Seram Trough to lie within part of a separate subducted plate, and the anomalous deep events to lie within a flattened deep part of the Java subduction zone.

The modeling predicts strains ranging from about 20% compression to nearly 50% extension, but the large extensional strains are associated with abrupt changes in the structure. The regions of generally uniform structure show mostly weak compression, about 10%. Most of the CMT mechanisms for the intermediate-depth events along the entire arc have lateral compression and downdip tension axes, but a few have downdip tension and normal compression axes (groups 1-5). Most deep events have downdip compression and normal tension axes (groups 7-9). All of the CMT mechanisms for events in the deformed westward dipping slab beneath the Banda Sea have downdip tension axes (groups 11 and 12). Some of these have normal compression axes, although lateral compression is more common.

Tonga-Kermadec Arc (Figure 18)

The Tonga and Kermadec Trenches form a remarkably linear boundary where the Pacific Plate subducts toward the west beneath the Indo-Australian Plate. The zone beneath Tonga is the most active deep earthquake zone in the world, and it is very well defined. The ISC-*pP* data in this study define an apparently continuous subducted plate with three PSBs. The geometry changes very rapidly along the arc, particularly below about 400 km depth. The structure delineated in this study is nearly identical to that found by *Billington* [1980].

The Niuafo'ou Fracture Zone truncates the Tonga subduction zone at its northern end near TK1, which corresponds to a tear proposed by *Yamaoka et al.* [1986]. *Isacks et al.* [1969] and *Johnson and Molnar* [1972] presented evidence for hinge faulting in this region, separating the part of the Pacific Plate that subducts from the part that simply travels west on the northern side of the transform. The ISC-*pP* data indicate that the subducting plate bends toward the west into the transform, and some of the CMT focal mechanisms here could be interpreted as hinge faulting. The clear line of volcanoes ends just south of this bend, so it is difficult to say whether the few volcanoes near the bend are following it. The structure is fairly smooth and continuous in the upper 400 km of the plate, changing in dip from about 65°-70° beneath the Kermadec Trench to about 55°-60° beneath the Tonga Trench.

At depths greater than about 400 km, the structure beneath the Tonga Arc becomes greatly distorted. There is a "benchlike" (as *Billington* [1980] described it) structure extending laterally down the subducted plate from about 500 km depth beneath the northern Kermadec Trench to about 600 km depth beneath the southern Tonga Trench. Beneath the central Tonga Arc, the plate appears to curl under below about 400 km depth. *Louat and Dupont* [1982] suggested there were several independent slabs here separated by tears running laterally along the subducted plate. Although the ISC-*pP* data do not disprove this interpretation, we find no direct evidence for such segmentation, and thus prefer the simpler model. *Giardini and Woodhouse* [1984] have explained the contorted structure in this region as a result of shear deformation caused by flow in the mantle.

TK2 is a fairly well defined PSB, which crosses the trench obliquely just south of the distinct change in trench geometry occurring where the Louisville Ridge intersects the trench. There is little active volcanism along this part of the arc and there is no indication of any change in the volcanism. *Giardini and Woodhouse* [1984] suggest that this PSB might represent the extension of the Louisville Ridge which has been displaced to the south by shear flow in the mantle.

TK3 is a well defined PSB at the southern end of the Kermadec Trench just north of North Island, New Zealand, and marks the termination of the deep seismicity. Just south of TK3 there is an increase in the number of active volcanoes. Neither the Wadati-Benioff zone as defined by the ISC-*pP* data nor the volcanism extends farther south than North Island. *Reyners* [1983] used more detailed relocated seismicity data to delineate a possible tear near the northern terminus of the volcanism in this region.

Beneath the Fiordland region of South Island, New Zealand, microearthquake studies show that there is a Wadati-Benioff zone dipping steeply to the east [*Davey and Smith*, 1983; *Smith and Davey*, 1984], although there are no intermediate-depth events in the ISC-*pP* data in this region. A major strike-slip fault, the Alpine Fault, joins the westward dipping Tonga-Kermadec subduction zone to the eastward dipping subduction zone beneath Fiordland [*Scholz et al.*, 1973].

Although the complicated geometry of the contorted plate had to be simplified for modeling, the modeling predicts great variation in lateral strain, from 30% compression near the intersection of the Louisville Ridge and the Tonga and Kermadec Trenches, to 50% extension at the northern end of the Tonga Trench where it bends sharply to the west. The CMT data for northern Tonga show a strong predominance of downdip compressional mechanisms at all depths (groups 1-3). At depths less than about 400 km, most of these mechanisms have normal tension axes, but at depths greater than 400 km there is no clearly dominant orientation of tension axes. There are many anomalous mechanisms near the northern Tonga Arc, and several may indicate that hinge faulting occurs (groups 4 and 5). Intermediate-depth (group 6) and deep (group 7) events beneath the central part of this arc have compression axes dipping to the north or east, and tension axes dipping to the south or west. Events beneath North Island show downdip tension and normal or nearly lateral tension (group 8).

New Hebrides (Vanuatu) Arc (Figure 19)

Along the New Hebrides Trench, the Indo-Australian Plate subducts to the east beneath the Fiji Basin, where intermediate-depth seismicity extends to depths of 200-300 km with a dip of 65°-70°. There is also deep seismic activity beneath the Fiji Plateau which possibly connects to the New Hebrides subduction. The deep seismicity forms an almost horizontal plane with a slight dip toward the northwest. CMT focal mechanisms for these deep events have scattered tension axes, but most of the compression axes dip to the southwest (group 3). Some investigators have suggested that this deep seismicity occurs in a detached slab that remains from a

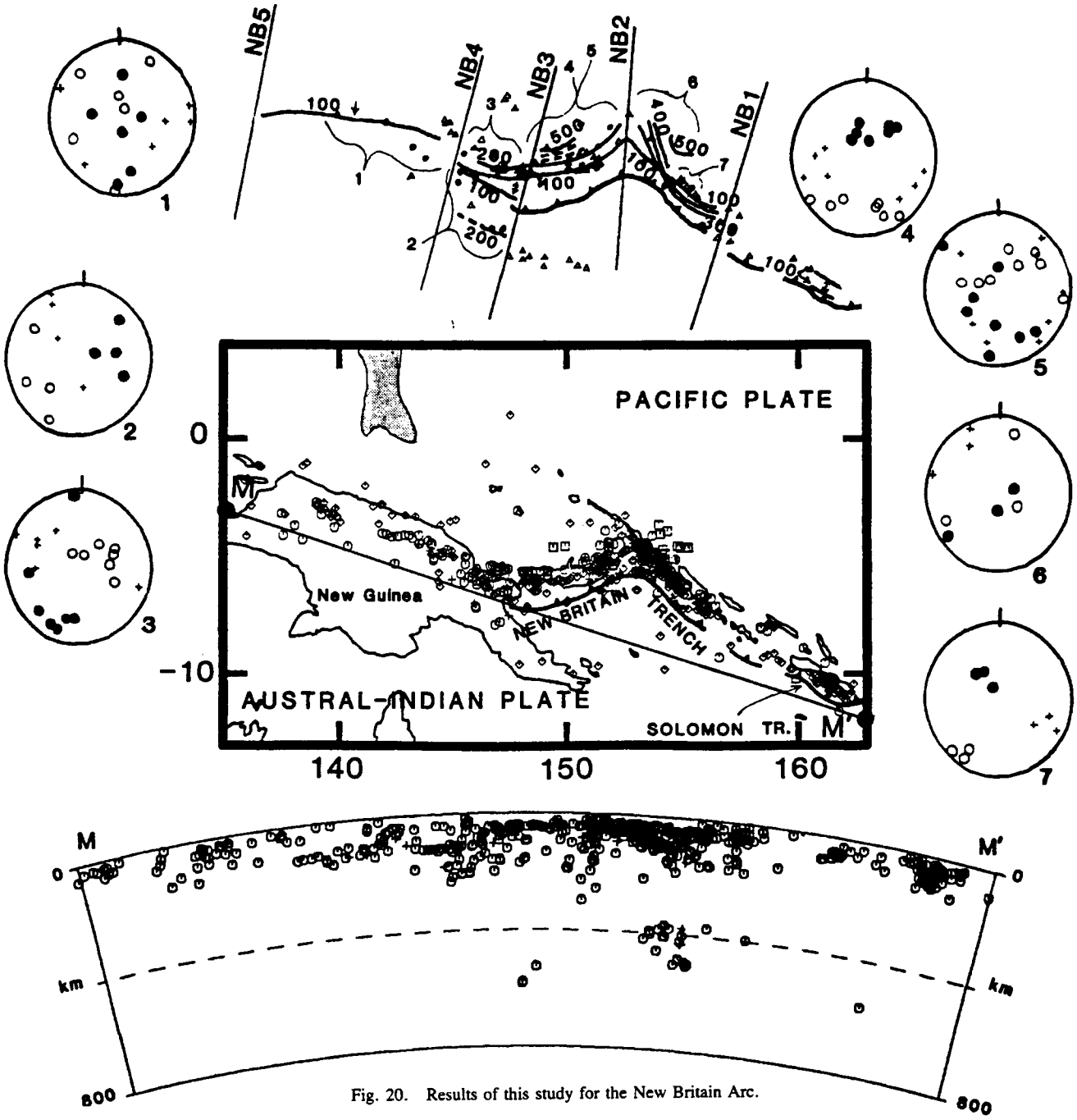

Fig. 20. Results of this study for the New Britain Arc.

previous subduction system [*Hanus and Vanek*, 1978, 1979, 1981], an idea strongly supported by ray propagation studies [*Barazangi et al.*, 1973]. Along most of the arc there is no seismic activity between about 300 and 550 km.

The southernmost PSB, NH5, marks the end of the intermediate-depth seismicity, as the trench bends around and terminates at the Hunter Fracture Zone. A line joining two volcanoes in this vicinity trends nearly east-west, which differs significantly from the orientation of the volcanic line farther north. NH4, although poorly defined, corresponds to a discontinuity in the Wadati-Benioff zone noted by *Louat et al.* [1982]. NH5 is well defined, and corresponds to the southern edge of a break in the trench where the D'Entrecasteaux Fracture Zone intersects the trench. Thus NH5 may correspond to a tear which *Chung and Kanamori* [1978*a*, *b*] associated with that feature. Both NH2 and NH1 are poorly defined; NH2 coincides with the end of the continuous line of active volcanism to the south, and NH1 corresponds to a discontinuity in the subducted plate noted by *Louat et al.*, [1982].

The east end of the South Solomon Trench is nearly parallel to the relative-motion vector and has virtually no intermediate-depth activity. This segment of trench is probably a trench-trench transform [*Isacks and Molnar*, 1971; *Johnson and Molnar*, 1972].

Modeling predicts large (50%) extensional strains at the southern end where the trench bends sharply to the east, and large (30%) compressional strains at the northern end where the trench has a slightly concave-seaward shape just before it bends toward its junction with the South Solomon Trench. In between, the strains are smaller (10-20%). Since the slab only

extends to a little over 200 km depth, the actual strains are probably much smaller, unless there is a direct connection between the intermediate and deep seismicity.

As noted by *Isacks and Molnar* [1971] and *Johnson and Molnar* [1972], there is a change in focal mechanisms across NH3, which corresponds to a tear proposed by *Yamaoka et al.* [1986]. This change in focal mechanisms reflects the change from compressional to extensional regimes. North of NH3 most of the CMT mechanisms have nearly vertical tension axes, and compression axes nearly horizontal and perpendicular to the trench (group 1). A few show lateral tension and downdip compression (group 4). The CMT focal mechanisms south of NH3 have nearly lateral tension and nearly normal compression axes with null axes oriented downdip (group 2). Many of the CMT focal mechanisms for events near NH4 and NH5 (group 5) are consistent with hinge faulting.

New Britain-New Guinea (Figure 20)

For the New Britain-New Guinea region, this study agrees with Johnson and *Molnar* [1972] and *Pascal* [1979]. The subduction in this region is not consistent with the motions of the major plates, and probably involves the interaction of several microplates, so it was impossible to predict the lateral strain in this region with the modeling method.

The New Britain Trench forms a sharp concave seaward cusp at NB2. Although the 100-km Wadati-Benioff zone contour appears to be continuous around the cusp, below 100 km there is no indication of continuity across this PSB. Just to the east of NB2 the Wadati-Benioff zone trends northwest-southeast and dips northeast to a depth of 400-500 km. At the northern end of this segment the dip is about 70°-75° toward the northeast, but steepens to vertical, then bends under so that at the southern end the seismic zone below about 100 km depth has a dip of about 80°-85° to the southwest. This distortion appears to be smooth, and forms an almost saddle-shaped Wadati-Benioff zone. The volcanoes above this segment all lie roughly above the 200-km contour, even where the slab appears to curl under. Both the intermediate and deep seismicity are terminated to the south by NB1.

Above the northern part of the Solomon Trench is a small cluster of intermediate-depth activity which appears to form two Wadati-Benioff zones dipping in opposite directions. The northward dipping leg extends to nearly 200 km depth and the southward dipping leg extends to only slightly over 100 km depth.

The Wadati-Benioff zone to the west of NB2 trends southwest and dips to the northwest at about 70°-75°. Seismicity extends to about 550 km depth, but a significant gap in activity occurs between about 300 and 500 km. The volcanoes to the west of the cusp do not form as clear a line as do those to the east.

To the west of NB3 the New Britain Trench intersects New Guinea and the seismicity again forms two planar zones, one dipping south and the other dipping north. The northward dipping zone extends to over 200 km depth and appears to be a continuous extension of the zone east of NB3. The zone dipping south extends to nearly 200 km depth. Mechanisms for events in the southward dipping zone have mostly downdip tension and normal compression axes, although there is considerable scatter (group 2). In the northward dipping zone the mechanisms also have mostly downdip tension and normal compression (group 3). There is only one volcano over the southward dipping seismic zone to the west of NB3. There is also a line of volcanoes east of NB3 which has no associated Wadati-Benioff zone.

Both the northward and southward dipping seismic zones terminate to the west against NB4. CMT mechanisms for two events near NB4 have nearly vertical compression axes, and null axes that are nearly horizontal and parallel to the PSB, which might indicate hinge faulting (group 2). West of this NB4 is a poorly defined shallow-dipping Wadati-Benioff zone dipping to the south, reaching a depth of about 150 km. There is a very large offset between this Wadati-Benioff zone and the southward dipping zone to the east of NB4. However, a line joining the one active volcano west of NB4 to the one east of NB4 is approximately parallel to the seismicity contours to the east of NB4, and is well to the south of the active seismicity.

Other Regions

Although this study attempted to evaluate all major regions of active subduction of oceanic lithosphere, there are several regions where there are intermediate and/or deep earthquakes which we did not discuss. In some regions, such as Hindu Kush and Burma, there is no subduction along an oceanic trench, so the modeling approach used in this study was inapplicable. In other regions, such as the Calabrian and Hellenic Arcs, the ISC-*pP* data were insufficient to delineate the Wadati-Benioff zone structure.

Beneath northern India (Hindu Kush) and Burma the ISC-*pP* data show Wadati-Benioff zones dipping northeast and east, respectively, to depths of 200-250 km, as indicated by previous investigators [*Fitch*, 1970; *Verma et al.*, 1976, 1980; *Roecker et al.*, 1980; *Chatelain et al.*, 1980]. The ISC-*pP* data are inadequate for delineating segmentation or other details of the structure in these regions.

In the Mediterranean region there is active subduction along both the Calabrian Arc of southern Italy [*Gasparini et al.*, 1982; *Bottari and Neri*, 1983] and the Hellenic Arc of Greece [*Makropoulos and Burton*, 1984]. There is also a nest of intermediate events near the Carpathian Arc in Romania [*Constantinescu and Enescu*, 1964; *Fuchs et al.*, 1979] which occasionally has very large events, most recently on March 4, 1977. However, in these regions, the ISC-*pP* data used in this study were insufficient to delineate definite Wadati-Benioff zones.

Near Granada, Spain, there is evidence for some intermediate-depth activity, which some investigators suggest may not be related to subduction [*Hatzfeld and Frogneux*, 1981]. *Chen and Molnar* [1983] have reviewed several other intercontinental areas where there is evidence for intermediate-depth earthquakes unrelated to subduction. Beneath Granada, two exceptionally deep events, one of magnitude 7.0 on March 29, 1954, and one of magnitude 4.0 in 1973, have been located at about 650 km depth [*Udias et al.*, 1976]. These events may occur within a relic slab remaining from a previous episode of subduction, but are probably not related to any current subduction.

APPENDIX

Modeling Subduction Geometries

The following is a step-by-step explanation of the geometric modeling method used to determine the lateral strain associated with both theoretical and observed subduction geometries.

1. We begin with a digitized representation of the trench geometry. For each point along the trench, we determine the local strike of the trench and assign a local dip measured perpendicular to the strike.

2. We rotate each point about the pole of rotation for the two convergent plates by an angle (A1) determined by the relative angular velocity of the two plates and the amount of time for subduction.

3. We rotate the new location of the point vertically by the dip angle about the tangent to the trench axis defined at the point's original location.

4. We perform these rotations five times, increasing the angle A1 by 2-million-year increments, to obtain a series of points which represent the path of the original point from the trench to its final position after 10 Ma of subduction.

5. Each point along the trench is subducted this way, independent of the points adjacent to it, to develop a set of subduction paths which together represent a model of the subducted plate.

Assumptions

The method assumes a thin spherical shell that is bent once at the trench axis, whereas actual plates have some thickness, and the major bend often occurs significantly inland of the trench axis. Another major assumption in the model is that the trench configuration remains constant with time. Although this assumption is not always true, this simple model is adequate in most cases. In some regions the tectonics are too complicated to adequately model this way.

Another assumption is that there is no significant strain in the direction of subduction. This may not be true since focal mechanisms in most regions indicate significant downdip stresses; however, it is the simplest assumption we can make to estimate the lateral strain. The lateral strain predicted by this modeling is not necessarily the maximum strain, nor the horizontal strain. It is the one-dimensional strain along the 10-Ma isochron between adjacent points that were originally at the trench at the same time.

Calculation of Lateral Strain

Since the model subducts each point along the trench independently in equal time increments, determination of the amount of lateral strain accommodated by the plate for a given geometry is straightforward. If the distance between points before subduction is d_0, and if the distance between points after subduction is d_1, the lateral strain is simply $S_1 = (d_0-d_1)/d_0$.

In this calculation, we fix the amount of time and the rate of subduction, rather than the length of slab subducted. Thus the modeled strain, S_1, is the strain expected after 10 Ma of subduction for each region, and the length of slab subducted varies from region to region.

Definition of Dip

One ambiguity in the modeling was the definition of the "dip" of the subducting plate. According to *Frank*'s [1968] argument, the subducted portion of a thin spherical shell should have the same curvature as the original surface, only in an opposite sense. Thus, for the theoretical curves in Figure 4, we define the dip as the angle between the tangents to the two surfaces at their point of intersection, which occurs at the trench (Figure 21).

For modeling observed subduction zones, this definition is imprecise. For observed Wadati-Benioff zones we define dip as the angle between the tangent to the surface of the earth at the trench and a line connecting the trench to the seismicity at a given depth, usually either the deepest seismicity, or the deepest intermediate depth seismicity (Figure 21). In some regions, such as South America, we use the deepest intermediate-depth seismicity, because the deep seismicity did not fit the structure defined by the intermediate depth seismicity.

Fig. 21. Definition of dip angle for (*a*) simple theoretical models used to produce Figure 5, and (*b*) observed subduction geometries.

Lateral Strain of Theoretical Geometries

We modeled numerous theoretical subduction geometries with constant arc radii and dips in order to produce the curves in Figure 4. Arc radius, as used throughout this paper, is measured by the angle subtended at the center of the earth by a radius of the small circle defined by the arc. For Figure 4, we used a pole of rotation about 90° from the midpoint of the trench such that at the midpoint, subduction was orthogonal. We rotated each point 10° (equivalent to 10 million years at 1°/Ma) to give downdip lengths of roughly 1100 km for the slabs. This length is as long as or longer than most seismically active Wadati-Benioff zones observed today, so the values of strain determined for these theoretical models should be considered maximum values.

Modeling Observed Subduction Zones

We applied this modeling technique to the major subduction zones of the circum-Pacific area. For each subduction zone, we digitized the trench axes at approximately 1° increments using GEBCO bathymetry maps. At each point we assigned dip angles which approximate the geometry delineated by the ISC-*pP* data. In some regions we chose the dips which simplify the observed structure somewhat. We defined the local tangent to the trench at each point by fitting a line through the points around it. We gave the point itself and the points on either side equal weight, and the next points on either side half-weight.

The poles and rotation angles are from *Minster and Jordan* [1978], except for the trenches bordering the Philippine Sea Plate, which are from *Seno* [1977]. We then determined the strain between each pair of points for 10 Ma of subduction as described above. We plotted the results of the modeling in maps and cross sections (Figures 9-20), showing the paths of the individual points as they were subducted, and the location of those points at 5 and 10 Ma.

Acknowledgments. We thank Chris Bennett for his development of the three-dimensional graphics software "FRAME3D." We also thank Wayne Pennington, John Sclater, Chuck Denham, and Richard Carlson for critical reviews of the manuscript. We thank Domenico Giardini and others at Harvard University for sending us a tape of their centroid moment tensor solutions, and the Smithsonian Institution for sending us

a tape of active volcanoes. This research was partially funded by NSF grant EAR-84-10352, and G. V. Burbach was supported during part of this time by funds provided for the Shell Foundation Distinguished Professorship of John G. Sclater at the University of Texas at Austin.

REFERENCES

Abe, K., Seismological evidence for a lithospheric tearing beneath the Aleutian Arc, *Earth Planet. Sci. Lett.*, *14*, 428-432, 1972.

Adamek, S., and W. Pennington, Microplate tectonics in the Panama region from seismicity studies (abstract), *Eos Trans. AGU*, *65*, 1109, 1984.

Adams, R. D., and B. G. Ferris, A further earthquake at exceptional depth beneath New Zealand, *N. Z. J. Geol. Geophys.*, *19*, 269-273, 1976.

Aoki, H., Plate tectonics of arc-junction at central Japan, *J. Phys. Earth*, *22*, 141-161, 1974.

Asudeh, I., I.S.C. mislocation of earthquakes in Iran and geometric residuals, *Tectonophysics*, *95*, 61-74, 1983.

Barazangi, M., B. L. Isacks, J. Oliver, J. Dubois, and G. Pascal, Descent of lithosphere beneath New Hebrides, Tonga-Fiji, and New Zealand: Evidence for detached slabs, *Nature*, *242*, 98-101, 1973.

Barazangi, M., and B. L. Isacks, Spatial distribution of earthquakes and subduction of the Nazca Plate beneath South America, *Geology*, *4*, 686-692, 1976.

Barazangi, M., and B. L. Isacks, Subduction of the Nazca Plate beneath Peru: Evidence from spatial distribution of earthquakes, *Geophys. J. R. Astron. Soc.*, *57*, 537-555, 1979*a*.

Barazangi, M., and B. L. Isacks, A comparison of the spatial distribution of mantle earthquakes determined from locations produced by local and by teleseismic networks for the Japan and Aleutian Arcs, *Bull. Seismol. Soc. Am.*, *69*, 1763-1770, 1979*b*.

Bennett, C., Frame 3-D: Interactive three-dimensional display of earthquake hypocenters, *Comput. Geosci.*, *11*, 249-277, 1985.

Bevis, M., and B. L. Isacks, Hypocentral trend surface analysis: Probing the geometry of Benioff zones, *J. Geophys. Res.*, *89*, 6153-6170, 1984.

Billington, S., The morphology and tectonics of the subducted lithosphere in the Tonga-Fiji-Kermadec region from seismicity and focal mechanism solutions, Ph.D. dissertation, Cornell Univ., Ithaca, New York, 1980.

Bottari, A., and G. Neri, Some statistical properties of a sequence of historical Calabro-Peloritan earthquakes, *J. Geophys. Res.*, *88*, 1209-1212, 1983.

Burbach, G. V., C. Frohlich, W. Pennington, and T. Matumoto, Seismicity and tectonics of the subducted Cocos Plate, *J. Geophys. Res.*, *89*, 7719-7735, 1984.

Cardwell, R. K., and B. L. Isacks, Geometry of the subducted lithosphere beneath the Banda Sea in eastern Indonesia from seismicity and fault plane solutions, *J. Geophys. Res.*, *83*, 2825-2838, 1978.

Cardwell, R. K., B. L. Isacks, and D. E. Karig, The spatial distribution of earthquakes, focal mechanism solutions, and subducted lithosphere in the Philippine and northeastern Indonesian Islands, in *The Tectonic and Geologic Evolution of Southeast Asian Seas and Islands, Part 1*, *Geophys. Monogr.*, vol. 23, edited by D. E. Hayes, pp. 1-35, AGU, Washington, D. C., 35p., 1980.

Carlson, R. L., Boundary forces and plate velocities, *Geophys. Res. Lett.*, *8*, 958-961, 1981.

Carr, M. J., R. E. Stoiber, and C. L. Drake, Discontinuities in the deep seismic zones under the Japanese arcs, *Geol. Soc. Am. Bull.*, *84*, 2917-2930, 1973.

Carr, M. J., W. I. Rose, and D. G. Mayfield, Potassium content of lavas and depth to the seismic zone in Central America, *Geotherm. Res.*, *5*, 387-401, 1979.

Chapple, W. M., and T. E. Tullis, Evaluation of the forces that drive the plates, *J. Geophys. Res.*, *82*, 1976-1984, 1977.

Chatelain, J. L., S. W. Roecker, D. Hatzfeld, and P. Molnar, Microearthquake seismicity and fault plane solutions in the Hindu Kush region and their tectonic implications, *J. Geophys. Res.*, *85*, 1365-1387, 1980.

Chen, W. P., and P. Molnar, Focal depths of intracontinental and intraplate earthquakes and their implications for the thermal and mechanical properties of the lithosphere, *J. Geophys. Res.*, *88*, 4183-4214, 1983.

Chung, W., and H. Kanamori, Subduction process of a fracture zone and aseismic ridges—the focal mechanisms and source characteristics of the New Hebrides earthquake of 1969 January 19 and some related events, *Geophys. J. R. Astron. Soc.*, *54*, 221-240, 1978*a*.

Chung, W., and H. Kanamori, A mechanical model for aseismic ridge subduction in the New Hebrides Arc, *Tectonophysics*, *50*, 29-40, *1978b*.

Constantinescu, L., and D. Enescu, Fault-plane solutions for some Roumanian earthquakes and their seismotectonic implications, *J. Geophys. Res.*, *69*, 667-674, 1964.

Cross, T. A., and R. H. Pilger, Jr., Controls of subduction geometry, location of magmatic arcs, and tectonics of arc and back-arc regions, *Geol. Soc. Am. Bull.*, *93*, 545-561, 1982.

Davey, F. J., and E. G. C. Smith, The tectonic setting of the Fiordland region, south-west New Zealand, *Geophys. J. R. Astron. Soc.*, *72*, 23-38, 1983.

Dean, B. W., and C. L. Drake, Focal mechanism solutions and tectonics of the Middle America Arc, *J. Geol.*, *86*, 111-128, 1978.

Dorel, J., Seismicity and seismic gap in the Lesser Antiles arc and earthquake hazard in Guadeloupe, *Geophys. J. R. Astron. Soc.*, *67*, 679-695, 1981.

Dzhibladze, E. A., "Deep" earthquake foci in the caucasus, *Izv. Acad. Sci. USSR Phys. Solid Earth*, Engl. Transl., *19*, 179-188, 1983.

Dziewonski, A. M., and J. H. Woodhouse, An experiment in systematic analysis of global seismicity: Centroid-moment tensor solutions for 201 moderate and large earthquakes of 1981, *J. Geophys. Res.*, *88*, 3247-3271, 1983.

Dziewonski, A. M., A. Friedman, D. Giardini, and J. H. Woodhouse, Global seismicity of 1982: Centroid-moment tensors for 308 earthquakes, *Phys. Earth Planet. Inter.*, *33*, 76-90, 1983*a*.

Dziewonski, A. M., A. Friedman, and J. H. Woodhouse, Centroid-moment tensors for January-March, 1983, *Phys. Earth Planet. Inter.*, *33*, 71-75, 1983*b*.

Dziewonski, A. M., J. E. Frazen, and J. H. Woodhouse, Centroid-moment tensors for April-June, 1983, *Phys. Earth Planet. Inter.*, *33*, 243-249, 1983.

Dziewonski, A. M., J. E. Frazen, and J. H. Woodhouse, Centroid-moment tensors for July-September, 1983, *Phys. Earth Planet. Inter.*, *34*, 1-8, 1984*a*.

Dziewonski, A. M., J. E. Frazen, and J. H. Woodhouse, Centroid-moment tensors for October-December, 1983, *Phys. Earth Planet. Inter.*, *34*, 129-136, 1984*b*.

Dziewonski, A. M., J. E. Frazen, and J. H. Woodhouse, Centroid-moment tensors for January-March, 1984, *Phys. Earth Planet. Inter.*, *34*, 209-219, 1984*c*.

Eguchi, T., S. Uyeda, and T. Maki, Seismotectonics and tectonic history of the Andaman Sea, *Tectonophysics*, *57*, 35-51, 1979.

Engdahl, E. R., Seismicity and plate subduction in the central Aleutians, in *Island Arcs, Deep Sea Trenches, and Back-Arc Basins*, *Maurice Ewing Ser.*, vol. 1, edited by M. Talwani and W. C. Pitman III, 259-271, AGU, Washington, D. C., 1977.

Fitch, T. J., Earthquake mechanisms in the Himalayan, Burmese, and Andaman regions and continental tectonics in central Asia, *J. Geophys. Res.*, *75*, 2699-2709, 1970.

Forsyth, D. W., Fault plane solutions and tectonics of the South Atlantic and Scotia Sea, *J. Geophys. Res.*, *80*, 1429-1443, 1975.

Forsyth, D. W., and S. Uyeda, On the relative importance of the driving forces of plate tectonics, *Geophys. J. R. Astron. Soc.*, *43*, 163-200, 1975.

Frank, F. C., Curvature of island arcs, *Nature*, *220*, 363, 1968.

Frankel, A., and W. R. McCann, Moderate and large earthquakes in the South Sandwich Arc: Indicators of tectonic variation along a subduction zone, *J. Geophys. Res.*, *84*, 5571-5577, 1979.

Frankel, A., W. R. McCann, and A. Murphy, Observations from a seismic network in the Virgin Islands region: Tectonic structures and earthquake swarms, *J. Geophys. Res.*, *85*, 2669-2678, 1980.

Fuchs, K. K., P. Bonjer, G. Bock, I. Cornea, C. Radu, D. Enescu, D. Jianu, A. Nourescu, G. Markler, T. Moldoveanu, and G. Tudorache, The Romanian earthquake of March 4, 1977, II, Aftershocks and migration of seismic activity, *Tectonophysics*, *53*, 225-247, 1979.

Fujita, K., and H. Kanamori, Double seismic zones and stresses of intermediate depth earthquakes, *Geophys. J. R. Astron. Soc.*, *66*, 131-156, 1981.

Furumoto, M., Spatio-temporal history of the deep Columbia earthquake of 1970, *Phys. Earth Planet. Inter.*, *15*, 1-12, 1977.

Gasparini, C., G. Iannaccone, P. Scandone, and R. Scarpa, Seismotectonics of the Calabrian arc, *Tectonophysics*, *84*, 267-286, 1982.

Giardini, D., Systematic analysis of deep seismicity: 200 centroid-moment tensor solutions for earthquakes between 1977 and 1980, *Geophys. J. R. Astron. Soc.*, *77*, 883-914, 1984.

Giardini, D., and J. H. Woodhouse, Deep seismicity and modes of deformation in Tonga subduction zone, *Nature*, *307*, 505-509, 1984.

Grange, F., P. Cunningham, J. Gagnepain, D. Hatzfeld, P. Molnar, L. Ocola, A. Rodrigues, S. W. Roecker, J. M. Stock, and G. Suarez, The configuration of the seismic zone and the downgoing slab in southern Peru, *Geophys. Res. Lett.*, *11*, 38-41, 1984*a*.

Grange, F., D. Hatzfeld, P. Cunningham, P. Molnar, S. W. Roecker, G. Suarez, A. Rodrigues, and L. Ocola, Tectonic implications of the microearthquake seismicity and fault plane solutions in southern Peru, *J. Geophys. Res.*, *89*, 6139-6152, 1984*b*.

Hager, B. H., and R. J. O'Connell, Kinematic models of large-scale flow in the earth's mantle, *J. Geophys. Res.*, *84*, 1031-1048, 1979.

Hager, B. H., R. J. O'Connell, and A. Raefsky, Subduction, back-arc spreading, and global mantle flow, *Tectonophysics*, *99*, 165-189, 1983.

Hamburger, M. W., and B. L. Isacks, Deep earthquakes in the southwest Pacific: Morphology and tectonic history (abstract), *Earthquake Notes*, *55*, 32, 1985.

Hamilton, W., Tectonics of the Indonesian region, *U.S. Geol. Surv. Prof. Pap.*, *1078*, 335 pp., 1979.

Hanus, V., and J. Vanek, Tonga-Lau system: Deep collision of subducted lithospheric plates, *J. Geophys.*, *44*, 473-480, 1978.

Hanus, V., and J. Vanek, Northern part of the Tonga region: A complicated subduction closure, *J. Geophys.*, *46*, 385-395, 1979.

Hanus, V., and J. Vanek, Plate tectonic interpretation of deep earthquakes between the Tonga-Lau and New Hebrides subduction zones, *Tectonophysics*, *75*, T19-T28, 1981.

Hasegawa, A., and I. S. Sacks, Subduction of the Nazca Plate beneath Peru as determined from seismic observations, *J. Geophys. Res.*, *86*, 4971-4980, 1981.

Hatzfeld, D., and M. Frogneux, Intermediate depth seismicity in the western Mediterranean unrelated to subduction of oceanic lithosphere, *Nature*, *292*, 443-445, 1981.

Hilde, T. W. C., and W. E. K. Warsi, Subduction induced rifting of the Nazca Plate along the Mendana Fracture zone (abstract), *Eos Trans. AGU*, *63*, 1113, 1982.

Hirahara, K., Three-dimensional seismic structure beneath southwest Japan: The subducting Philippine Sea Plate, *Tectonophysics*, *79*, 1-44, 1981.

Horiuchi, S., Deformation of sinking slab in consequence of absolute plate motion of island-side Izu-Bonin-Mariana Arc (in Japanese), *J. Seismol. Soc. Jpn.*, *30*, 435-447, 1977.

Isacks, B. L., and M. Barazangi, Geometry of Benioff zones: Lateral segmentation and downwards bending of the subducted lithosphere, in *Island Arcs, Deep Sea Trenches, and Back-Arc Basins, Maurice Ewing Ser.*, vol. 1, edited by M. Talwani and W. C. Pitman III, pp. 99-114, AGU, Washington, D. C., 1977.

Isacks, B. L., and P. Molnar, Distribution of stresses in the descending lithosphere from a global survey of focal mechanism solutions of mantle earthquakes, *Rev. Geophys.*, *9*, 103-174, 1971.

Isacks, B. L., L. R. Sykes, and J. Oliver, Focal mechanisms of deep and shallow earthquakes in the Tonga-Kermadec region and the tectonics of island arcs, *Geol. Soc. Am. Bull.*, *80*, 1443-1470, 1969.

Jacob, K. H., K. Nakamura, and J. N. Davies, Trench-volcano gap along the Alaska-Aleutian Arc: Facts, and speculations on the role of terrigenous sediments for subduction, in *Island Arcs, Deep Sea Trenches, and Back-Arc Basins, Maurice Ewing Ser.*, vol. 1, edited by M. Talwani and W. C. Pitman III, pp. 243-258, AGU, Washington, D. C., 1977.

Johnson, T., and P. Molnar, Focal mechanisms and plate tectonics of the southwest Pacific, *J. Geophys. Res.*, *77*, 5000-5032, 1972.

Kanamori, H., Focal mechanism of the Tokachi-Oki earthquake of May 16, 1968: Contortion of the lithosphere at the junction of two trenches, *Tectonophysics*, *12*, 1-13, 1971.

Katsumata, M., Seismic activities in and near Japan: I. Distribution of epicenters of earthquakes in an near Japan, *J. Seismol. Soc. Jpn.*, *19*, 237-245, 1966.

Katsumata, M., and L. R. Sykes, Seismicity and tectonics of the western Pacific: Izu-Mariana-Caroline and Ryukyu-Taiwan regions, *J. Geophys. Res.*, *74*, 5923-5948, 1969.

Kawakatsu, H., and T. Seno, Triple seismic zone and the regional variation of seismicity along the northern Honshu Arc, *J. Geophys. Res.*, *88*, 4215-4230, 1983.

Kelleher, J., and W. McCann, Buoyant zones, great earthquakes, and unstable boundaries of subduction, *J. Geophys. Res.*, *81*, 4885-4896, 1976.

LeFevre, L. V., and K. C. McNally, Stress distribution and subduction of aseismic ridges in the Middle America subduction zone, *J. Geophys. Res.*, *90*, 4495-4510, 1985.

Liaw, H. B., Modified regularization method applied to join determination of hypocenters and velocity structure and its application to earthquake data from northern Costa Rica, Ph.D. dissertation, Univ. of Texas, Dallas, 1982.

Louat, R., and J. Dupont, Seismicite de l'arc des Tonga-Kermadec, in *Contribution a l'etude geodynamique du sud-ouest Pacifique*, pp. 299-317, Office de la Recherche Scientifique et Technique Outre-Mer, Paris, 1982.

Louat, R., J. Daniel, and B. Isacks, Seismicite de l'arc des Nouvelles-Hebrides, in *Contribution a l'etude geodynamique du sud-ouest Pacifique*, pp. 111-148, Office de la Recherche Scientifique et Technique Outre-Mer Paris, 1982.

McLaren, J. P., and C. Frohlich, Model calculations of regional network locations for earthquakes in subduction zones, *Bull. Seismol. Soc. Am.*, *75*, 397-413, 1985.

Makropoulos, K. C., and P. W. Burton, Greek tectonics and seismicity, *Tectonophysics*, *106*, 275-304, 1984.

Matumoto, T., G. Latham, and J. Ulmana, Seismicity studies in northern Costa Rica (abstract), *Eos Trans. AGU*, *57*, 290, 1976.

McCann, W. R., and L. R. Sykes, Subduction of aseismic ridges beneath the Caribbean Plate: Implications for the tectonics and seismic potential of the northeastern Caribbean, *J. Geophys. Res.*, *89*, 4493-4519, 1984.

Minamino, T., and N. Fujii, The effect of the contorted "nose" of a subducting slab on the stress field in the continental lithosphere at an arc-arc junction, *Geophys. J. R. Astron. Soc.*, *67*, 145-158, 1981.

Minster, J. B., and T. H. Jordan, Present day plate motions, *J. Geophys. Res.*, *83*, 5331-5354, 1978.

Molnar, P., and L. R. Sykes, Tectonics of the Caribbean and Middle America regions from focal mechanisms and seismicity, *Geol. Soc. Am. Bull.*, *80*, 1639-1684, 1969.

Murphy, A. J., and W. R. McCann, Preliminary results from a new seismic network in the northeastern Caribbean, *Bull. Seismol. Soc. Am.*, *69*, 1497-1513, 1979.

Nixon, G. T., The relationship between Quaternary volcanism in central Mexico and the seismicity and structure of subducted ocean lithosphere, *Geol. Soc. Am. Bull.*, *93*, 514-523, 1982.

Papp, Z., A three-dimensional model of the seismicity in the Banda Sea region, *Tectonophysics*, *69*, 63-83, 1980.

Pascal, G., Seismotectonics of the Papua New Guinea-Solomon Islands region, *Tectonophysics*, *57*, 7-34, 1979.

Pennington, W. D., Subduction of the eastern Panama Basin and seismotectonics of northwestern South America, *J. Geophys. Res.*, *86*, 10,753-10,770, 1981.

Pilger, R. H., Plate reconstructions, aseismic ridges, and low-angle subduction beneath the Andes, *Geol. Soc. Am. Bull.*, *92*, 448-456, 1981.

Pulpan, H., and C. Frohlich, Geometry of the subducted plate near Kodiak Island and lower Cook Inlet, Alaska, determined from relocated earthquake hypocenters, *Bull. Seismol. Soc. Am.*, *75*, 791-810, 1985.

Reyners, M., Lateral segmentation of the subducted plate at the Hikurangi margin, New Zealand, *Tectonophysics*, *96*, 203-223, 1983.

Reyners, M., and K. S. Coles, Fine structure of the dipping seismic zone and subduction mechanics in the Shumagin Islands, Alaska, *J. Geophys. Res.*, *87*, 356-366, 1982.

Roecker, S. W., O. V. Soboleva, I. L. Nersesov, A. A. Lukk, D. Hatzfeld, J. L. Chatelain, and P. Molnar, Seismicity and fault plane solutions of intermediate depth earthquakes in the Pamir-Hindu Kush region, *J. Geophys. Res.*, *85*, 1358-1364, 1980.

Sasatani, T., Mechanism of mantle earthquakes near the junction of the Kurile and the northern Honshu arcs, *J. Phys. Earth*, *24* 341-354, 1976.

Schneider, J. F, The intermediate-depth microearthquakes of the Bacaramanga rest, Columbia, Ph.D. dissertation, Univ. of Wisconsin, Madison, Wisconsin, 1984.

Scholz, C. H., J. M. W. Rynn, R. W. Reed, and C. Frohlich, Detailed seismicity of the Alpine Fault zone, Fiordland region, New Zealand, *Geol. Soc. Am. Bull.*, *84*, 3297-3316, 1973.

Seno, T., The instantaneous rotation vector of the Philippine Sea Plate relative to the Eurasian Plate, *Tectonophysics*, *42*, 209-226, 1977.

Shiono, K., T. Mikumo, and Y. Ishikawa, Tectonics of the Kyushu-

Ryukyu Arc as evidenced from seismicity and focal mechanism of shallow to intermediate-depth earthquakes, *J. Phys. Earth*, *28*, 17-43, 1980.

Shreve, R. L., and M. Cloos, Dynamics of sediment subduction, melange formation, and prism accretion, *J. Geophys. Res.*, in press, 1986.

Smith, E. G. C., and F. J. Davey, Joint hypocenter determination of intermediate depth earthquakes in Fiordland, New Zealand, *Tectonophysics*, *104*, 127-144, 1984.

Spence, W., The Aleutian Arc: Tectonic blocks, episodic subduction, and magma generation, *J. Geophys. Res.*, *82*, 213-230, 1977.

Stark, P. B., and C. Frohlich, The depths of the deepest deep earthquakes, *J. Geophys. Res.*, *90*, 1859-1869, 1985.

Stauder, W., Fault motion and spatially bounded character of earthquakes in Amchitka Pass and the Delarof Islands, *J. Geophys. Res.*, *77*, 2072-2080, 1972.

Stauder, W., and L. Mualchin, Fault motion in the larger earthquakes of the Kuril-Kamchatka Arc and of the Kurile-Hokkaido corner, *J. Geophys. Res.*, *81*, 297-308, 1976.

Stein, S., J. F. Engeln, D. A. Wiens, K. Fujita, and R. C. Speed, Subduction seismicity and tectonics in the lesser Antilles Arc, *J. Geophys. Res.*, *87*, 8642-8664, 1982.

Stoiber, R. E., and M. J. Carr, Quaternary volcanic and tectonic segmentation of Central America, *Bull. Volcanolo.*, *37*, 304-325, 1973.

Strobach, K., Curvature of island arcs and plate tectonics, *Z. Geophys.*, *39*, 819-831, 1973.

Swift, S. A., and M. J. Carr, The segmented nature of the Chilean seismic zone, *Phys. Earth Planet. Inter.*, *9*, 183-191, 1974.

Tovish, A., and G. Schubert, Island arc curvature, velocity of convergence, and angle of subduction, *Geophys. Res. Lett.*, *5*, 329-332, 1978.

Udias, A., A. L. Arroyo, and J. Mezcua, Seismotectonics of the Azores-Alboran region, *Tectonophysics*, *31*, 259-289, 1976.

Umino, N., and A. Hasegawa, A detailed structure of the deep seismic zone and earthquake mechanism in the northeastern Japan arc, (in Japanese), *J. Seismol. Soc. Jpn.*, *35*, 237-257, 1982.

Utsu, T., Seismological evidence for anomalous structure of island arcs, with special reference to the Japanese region, *Rev. Geophys.*, *9*, 839-890, 1971.

Utsu, T., Space-time pattern of large earthquakes occurring off the Pacific coast of the Japanese islands, *J. Phys. Earth*, 22, 325-342, 1974.

Vassiliou, M. S., The state of stress in subducting slabs as revealed by earthquakes analysed by moment tensor inversion, *Earth Planet. Sci. Lett.*, *69*, 195-202, 1984.

Vassiliou, M. S., B. H. Hager, and A. Raefsky, The distribution of earthquakes with depth and stress in subducting slabs, *J. Geodyn.*, *1*, 11-28, 1984.

Veith, K. F., The relationship of island arc seismicity to plate tectonics, Ph.D. dissertation, Southern Methodist Univ., Dallas, Texas, 1974.

Verma, R. K., M. Mukhopadhyay, and M. S. Ahluwalia, Earthquake mechanisms and tectonic features of northern Burma, *Tectonophysics*, 32, 387-399, 1976.

Verma, R. K., M. Mukhopadhyay, and A. K. Bhanja, Seismotectonics of the Hindukush and Bakuchistan arc, *Tectonophysics*, *66*, 301-322, 1980.

Vogt, P. R., A. Lowrie, D. Bracey, and R. Hey, Subduction of aseismic oceanic ridges: Effects on shape, seismicity, and other characteristics of consuming plate boundaries, *Spec. Pap., Geol. Soc. Am.*, *172*, 59 pp., 1976.

Warsi, W. E. K., T. W. C. Hilde, and R. C. Searle, Convergence structures of the Peru Trench between 10°S and 14°S, *Tectonophysics*, *99*, 313-329, 1983.

Yamaoka K., Y. Fukao, and M. Kumazawa, Spherical shell tectonics: Effects of sphericity and inextensibility on the geometry of the descending lithosphere, *Rev. of Geophys.*, *24*, 127-53, 1986.

G. V. Burbach, Shell Western E. & P., Inc., P.O. Box 576, Houston, Texas 77001.

C. Frohlich, Institute for Geophysics, University of Texas at Austin, 4920 North I.H. 35, Austin, Texas 78751.

(Received February 3, 1986;
accepted May 29, 1986.)